MCB
Journals.ASM.org

The Prolyl Isomerase Pin1 Targets Stem-Loop Binding Protein (SLBP) To Dissociate the SLBP-Histone mRNA Complex Linking Histone mRNA Decay with SLBP Ubiquitination

Nithya Krishnan,[a] TuKiet T. Lam,[c] Andrew Fritz,[d] Donald Rempinski,[a] Kieran O'Loughlin,[e] Hans Minderman,[e] Ronald Berezney,[d] William F. Marzluff,[f] and Roopa Thapar[a,b]

Hauptman Woodward Medical Research Institute[a] and Department of Structural Biology,[b] SUNY at Buffalo, Buffalo, New York, USA; W. M. Keck Foundation Biotechnology Resource Laboratory, Yale University, New Haven, Connecticut, USA[c]; Department of Biological Sciences, SUNY at Buffalo, Buffalo, New York, USA[d]; Department of Flow and Image Cytometry, Roswell Park Cancer Institute, Buffalo, New York, USA[e]; and Department of Biochemistry and Biophysics, University of North Carolina at Chapel Hill, Chapel Hill, North Carolina, USA[f]

Histone mRNAs are rapidly degraded at the end of S phase, and a 26-nucleotide stem-loop in the 3′ untranslated region is a key determinant of histone mRNA stability. This sequence is the binding site for stem-loop binding protein (SLBP), which helps to recruit components of the RNA degradation machinery to the histone mRNA 3′ end. SLBP is the only protein whose expression is cell cycle regulated during S phase and whose degradation is temporally correlated with histone mRNA degradation. Here we report that chemical inhibition of the prolyl isomerase Pin1 or downregulation of Pin1 by small interfering RNA (siRNA) increases the mRNA stability of all five core histone mRNAs and the stability of SLBP. Pin1 regulates SLBP polyubiquitination via the Ser20/Ser23 phosphodegron in the N terminus. siRNA knockdown of Pin1 results in accumulation of SLBP in the nucleus. We show that Pin1 can act along with protein phosphatase 2A (PP2A) *in vitro* to dephosphorylate a phosphothreonine in a conserved TPNK sequence in the SLBP RNA binding domain, thereby dissociating SLBP from the histone mRNA hairpin. Our data suggest that Pin1 and PP2A act to coordinate the degradation of SLBP by the ubiquitin proteasome system and the exosome-mediated degradation of the histone mRNA by regulating complex dissociation.

The prolyl isomerase Pin1 has diverse effects on cellular metabolism that include control of the cell cycle, regulation of cell differentiation, proliferation, and genomic stability (11, 36, 38, 64). Pin1 catalyzes *cis-trans* prolyl isomerization in its substrates, facilitating conformational changes that regulate protein function. Proteins identified as Pin1 targets include mitotic phosphoproteins (4, 17, 60), transcription factors (14, 34, 49), and cell cycle regulators (46, 63). Pin1 is specific for phosphorylated Ser/Thr-Pro sequences and acts along with kinases and phosphatases to exert its biochemical effects.

Pin1 plays an essential role in regulating transcription initiation, elongation, and termination (61, 62). In both yeast and mammals, Pin1 (Ess1 in yeast) regulates the conformation and phosphorylation state of the RNA polymerase (RNAP) II carboxy-terminal domain (CTD) (1, 41). Ess1 promotes dephosphorylation of Ser-5 of the heptad repeat (Y-S^2-P-T-S^5-P-S) in the CTD by interactions with CTD-associated phosphatases Ssu72 and Pcf11, thereby regulating the association of the CTD with components of the 3′-end processing machinery (24, 56). Yeast Ess1 is required for transcription termination of small noncoding RNAs such as snoRNAs, cryptic unstable transcripts (CUTs), and upstream regulatory RNAs (uRNAs) via the Nrd1 pathway (51). Ess1 functionally interacts with the transcription initiation factor TFIIB, Ssu72 phosphatase, and Pta1 components of the 3′-end processing machinery to influence gene looping (24). Besides its effects on transcription, Pin1 has been implicated in the control of mRNA stability of three AU-rich element (ARE)-containing mRNAs, namely, those for granulocye-macrophage colony-stimulating factor (GM-CSF), parathyroid hormone (*Pth*), and transforming growth factor β (TGF-β), in the cytoplasm (10, 25). These effects are mediated via direct association of Pin1 with phosphorylated forms of the ARE-binding proteins AUF1 and KSRP. Pin1 promotes dephosphorylation of AUF1 and KSRP *in vivo*, regulating their interactions with the ARE sequences in the 3′ untranslated regions (UTRs) of the respective mRNAs.

Histone mRNAs are a unique set of eukaryotic transcripts that accumulate primarily during S phase (40). They are the only eukaryotic cellular mRNAs that are not polyadenylated, ending instead in a conserved stem-loop. These mRNAs have very short half-lives, approximately 40 min and 10 min during and at the end of S phase, respectively (2, 15). Stem-loop binding protein (SLBP) is a histone mRNA-specific processing factor that binds the stem-loop at the 3′ end of histone mRNA. The SLBP-histone mRNA complex functions as a coordinate unit in all steps of histone mRNA metabolism. SLBP is the only protein involved in histone mRNA metabolism whose expression during S phase is temporally correlated to that of histone mRNAs.

In this study, we use an integrated nuclear magnetic resonance (NMR), biochemical, and biological approach to show that the prolyl isomerase activity of Pin1 regulates the SLBP-histone

Received 20 March 2012 **Returned for modification** 18 April 2012
Accepted 13 August 2012
Published ahead of print 20 August 2012
Address correspondence to Roopa Thapar, rthapar@hwi.buffalo.edu.
N.K. and R.T. contributed equally to this article.
Supplemental material for this article may be found at http://mcb.asm.org/.

doi:10.1128/MCB.00382-12

mRNA complex. We have recently shown that SLBP undergoes proline isomerization about a conserved phosphorylated Thr-Pro sequence in its RNA binding domain (RBD) (3, 29, 65). There are six Ser-Pro/Thr-Pro sequences in human SLBP, all of which have been previously shown to be phosphorylated by mass spectrometry (12). We confirmed the existence of these additional phosphorylation sites by mass spectrometry and show that multisite phosphorylation at the N terminus at either Ser7, Ser20, Ser23, Thr60, or Thr61 in addition to Thr171 in the RNA binding domain is required for efficient interaction of SLBP with Pin1. We also mapped the binding site on Pin1 for SLBP by NMR spectroscopy and confirmed that Pin1 interacts with a conserved phospho-Thr171-Pro172 sequence in the SLBP RBD. We show that Pin1 and protein phosphatase 2A (PP2A) play an important role in dissociating SLBP from the histone mRNA 3′ end. Moreover, when Pin1 was downregulated by small interfering RNA (siRNA) or the prolyl isomerase activity of Pin1 was inhibited, we observed an increase in SLBP stability, increased accumulation of polyubiquitinated SLBP, and an increase in the abundance of histone mRNAs that was directly attributed to decreased rates of mRNA decay.

Our results suggest that at the end of S phase, SLBP is likely dephosphorylated at T171 by Pin1 and PP2A to trigger dissociation of SLBP from the histone mRNA. This facilitates histone mRNA decay in the cytoplasm, and the free SLBP likely relocalizes to the nucleus, facilitating SLBP ubiquitination and degradation. Therefore, Pin1 and PP2A work to intersect two major pathways of gene expression at the end of S phase, namely, the degradation of SLBP by the ubiquitin proteasome system and the exosome-mediated degradation of the histone mRNA by regulating complex dissociation.

MATERIALS AND METHODS

Protein and RNA constructs. Full-length and SLBP RNA binding and processing domains (RPDs) were subcloned into the NcoI and XhoI restriction sites of the baculovirus vector pFastBacHTA and were expressed using the Bac-to-Bac expression system (Invitrogen) previously described (7). Sf21 cells were infected with baculovirus (at a density of 5×10^5 cells/ml) in serum-free SF900 medium (Gibco) and purified using standard protocols using nickel affinity chromatography. Phosphorylation of all proteins was confirmed by high-resolution tandem mass spectrometry at the Keck MS and Proteomics Resource at Yale University (T. T. Lam and R. Thapar, unpublished data). The samples were concentrated and buffer exchanged using a G25 column into NMR buffer or phosphate-buffered saline (PBS) for the dissociation assays. Human Pin1 was expressed as a glutathione *S*-transferase (GST) fusion protein and purified by glutathione (GSH) affinity chromatography using a HiTrap GST column (GE) for the NMR chemical shift mapping experiments. The GST was cleaved with biotinylated thrombin, and the residual thrombin was removed using streptavidin beads. The cleaved and uncleaved proteins were separated by putting the mixture over a second glutathione (GSH)-bead column. The protein was further cleaned up on an S200 Superdex column (GE). Uniformly ^{15}N-labeled Pin1 was made by growing bacteria in minimal medium with $^{15}NH_4Cl$ as the sole source of nitrogen and purified as described above. Pin1 was expressed from the vector pET28a for the dissociation experiments and was purified using nickel affinity and gel filtration chromatographies. Threonine-phosphorylated and unphosphorylated peptides corresponding to residues His161-Arg180 (^{161}HLRQ PGIHPKTPNKFKKYSR^{180}) of human SLBP were synthesized by Sigma-Genosys. The SFTpTP peptide (made at the UNC peptide core facility) has a single phosphate on Thr61 and corresponds to residues 54 to 68 (^{54}RR PESFTTPEGPKPR^{68}) from the N terminus of human SLBP (hSLBP). All peptides were at least 90% pure as determined by reverse-phase high-performance liquid chromatography (HPLC) and matrix-assisted laser desorption ionization–mass spectrometry (MALDI-MS). The stem-loop RNAs, labeled with fluorescein at either the 5′ or 3′ end, were synthesized by Dharmacon, Inc. The RNA was folded by heating at 95°C for 2 min and snap-cooled on ice for 10 min to ensure the lowest-energy hairpin conformer.

Antibodies and reagents. Rabbit polyclonal anti-Pin1, mouse monoclonal antihemagglutinin (anti-HA), and goat anti-SC-35 antibodies were obtained from Santa Cruz; an in-house rabbit polyclonal anti-SLBP antibody made toward the C terminus of human SLBP was used for the Western blots; and goat polyclonal anti-SLBP (Santa Cruz Antibodies) was used in the ImageStream (IS) flow cytometry experiments. For immunofluorescence experiments, a rabbit monoclonal antibody toward Pin1 (Abcam) was used and a mouse monoclonal antibody toward HA (Abcam) was used. Antibodies toward the following proteins were purchased from Bethyl Laboratories: eukaryotic initiation factor 4G1 (eIF4G1), eIF4E, CPSF73, CPSF100, CPSF160, CPSF30, actin, symplekin, CSTF64, and Myc. Rabbit polyclonal antibody for histone H3 was purchased from Abcam. Anti-Flag biotinylated M2 monoclonal antibody was purchased from Sigma. Purified PP2A and PP1 protein Ser/Thr phosphatases were obtained from Biomol and NEB, respectively. The Pin1 inhibitor PiB (diethyl-1,3,6,8-tetrahydro-1,3,6,8-tetraoxobenzol-phenanthroline-2,7-diacetate) was purchased from Sigma and resuspended in dimethyl sulfoxide (DMSO). The proteasome inhibitor *N*-acetyl-Leu-Leu-Nle-CHO (ALLN) was purchased from Calbiochem.

Pin1 RNA interference (RNAi). HeLa cells were cultured in Dulbecco's modified Eagle medium (DMEM) with 10% fetal bovine serum. Pin1 siRNA and control C2 RNAs were obtained from Dharmacon's ON-TARGETplus siRNA collection (catalog number 003291), and the knockdown was performed using Lipofectamine RNAiMax (Invitrogen) using a two-hit method (55). We used either a single siRNA corresponding to the sequence 5′-GCUCAGGCCGAGUGUACUAA-3′ or a pool of four different siRNAs from the ON-TARGETplus SMARTpool siRNA collection (the sequences are 5′-CCACAUCACUAACGCCAGC-3′, 5′-GAAGAUCACCCGGACCAAG-3′, 5′-GAAGACGCCUCGUUUGCGC-3′, and 5′-GCUCAGGCCGAGUGUACUA-3′). Similar effects were observed irrespective of whether a single siRNA or the pool of four different siRNAs was used, indicating that the off-target effects were minimal. The second siRNA transfection was performed 48 h after the first hit, and the cells were cultured for another 72 h before harvesting for microarray analysis or reverse transcription-PCR (RT-PCR).

Isolation of total RNA for RT-PCR. HeLa cells were lysed in 1 ml of TRIzol reagent (Invitrogen). The homogenized sample was incubated for 5 min at room temperature to permit complete dissociation of nucleoprotein complexes. Two hundred microliters of chloroform was added per 1 ml of TRIzol reagent, mixed vigorously, and allowed to sit at room temperature for 2 to 3 min. The samples were centrifuged at 12,000 × *g* for 15 min at 4°C. Centrifugation separated the biphasic mixtures into the lower red phenol-chloroform phase and the upper colorless aqueous phase. RNA was precipitated from the upper aqueous phase using 1 ml of isopropanol. The samples were centrifuged at 12,000 × *g* for 10 min at 4°C. The RNA pellet was washed once with 2 ml of 75% ethanol, air dried, and redissolved in 25 μl of diethyl pyrocarbonate (DEPC)-treated water. Total RNA obtained was purified using PureLink Micro-to-Midi RNA purification system (Invitrogen) as per the manufacturer's instructions. All RNA samples used for RT-PCR had a ratio of optical densities (OD) at 260 and 280 nm of 1.9 to 2.0 (NanoDrop).

Quantitative RT-PCR. Real-time quantitative reverse transcription-PCR (qRT-PCR) was performed using a Bio-Rad MyiQ single-color real-time PCR system. The cDNAs were synthesized from 1.5 μg of total RNA using SuperScript III reverse transcriptase (200 U/μl) (Invitrogen) with random hexamers as per the manufacturer's instructions. The primers were designed using the program Primer3 (http://frodo.wi.mit.edu/primer3/) and are summarized in Table S1 in the supplemental material. The real-time PCR primers were synthesized by Integrated DNA Technol-

ogies (IDT), Coralville, IA (see Table S1 in the supplemental material). The reaction components were added as follows to the indicated final concentrations: 2.5 μl of water, 4.5 μl of forward primer (5 μM), 4.5 μl of reverse primer (5 μM) 12.5 μl of SYBR green (Applied Biosystems), and 1 μl of cDNA. The cycling profile for each run was 50°C for 2 min, 95°C for 10 min, and 40 cycles of 95°C for 15 s, followed by 60°C for 10 min, using the default ramp rate. The change in gene expression levels was determined by normalizing mRNA levels of the gene of interest to the mRNA level of the housekeeping gene, the glyceraldehyde-3-phosphate dehydrogenase (GAPDH) gene, using the comparative threshold cycle (C_T) method. Several controls were also performed to determine whether the change in histone mRNA levels in response to Pin1 siRNA treatment could be rescued. Control and siRNA-treated HEK293 cells were transiently transfected with wild-type Pin1 (Pin1 WT), the Pin1 W34A mutant, SLBP WT, or the SLBP T171A or SLBP T171E mutant 48 h after the second hit for an additional 24 h. The total mRNA levels were determined as described above.

FACS and IS flow cytometry. HeLa cells were collected and washed in cold PBS, resuspended in PBS, and fixed in chilled ethanol overnight. Cells were then washed and resuspended in PBS with propidium iodide (PI) for 30 min at 37°C. DNA content was measured by flow cytometry (fluorescence-activated cell sorting [FACS]) and analyzed in Modfit. IS flow cytometry was performed using IS100 (Amnis) on HeLa cells that were stained for anti-SLBP fluorescein isothiocyanate (FITC) and DRAQ5 for nuclear imaging. A total of 5,000 events were collected for both control and Pin1 siRNA-treated cells. The cell populations were gated for single cells that were in focus and were positive for both DRAQ5 and anti-SLBP FITC. The spatial relationship between SLBP and DRAQ5 was measured using the "Similarity" feature in the IDEAS software package. The similarity score (SS) is a log-transformed Pearson's correlation coefficient between the pixel values of two image pairs, which provides a measure of the degree of nuclear localization of SLBP by measuring the pixel intensity correlation between the SLBP and DRAQ5 (nuclear dye) images. Cells with low SSs exhibit no correlation between the images, whereas cells with high SSs exhibit a positive correlation between the images.

Coimmunoprecipitation and Western blot analysis. HeLa cells were cultured in DMEM with 10% fetal bovine serum. HeLa cell extract was prepared from 1×10^7 cells. Cells were lysed in NP-40 lysis buffer and spun at 13,000 × *g* for 10 min at 4°C. The lysate was probed for the protein under investigation by Western blotting with enhanced chemiluminescence (ECL). For the coimmunoprecipitation studies, HeLa cells stably expressing HA-SLBP were cultured in DMEM with 10% fetal bovine serum. Total cell extract was prepared from 1×10^7 cells. Cells were lysed, and the lysate was precleared and then incubated either with an anti-Pin1 antibody or anti-Myc (as a control), 50 μl of protein A/G Plus beads (Santa Cruz Antibodies), and 10 μg/ml RNase A where indicated, overnight at 4°C. The next day, the beads were washed five times with lysis buffer with end-over mixing for 1 min, followed by spinning of the beads at 3,000 × *g* for 1 min at 4°C for each wash. The bound proteins were resolved on a 15% SDS-PAGE gel and probed for Pin1 or the HA tag by Western blotting with ECL. For coimmunoprecipitation of Pin1 with SLBP mutants, Flag-tagged SLBP wild-type and SLBP T60A/T61A, T171A, T60A/T61A/T171A, S7A, S20A/S23A, and S20A/S23A/T171A mutants were cloned into vector pcDNA3.1 and transiently transfected into HeLa cells. Cells were harvested after 48 h. The cells were immunoprecipitated using anti-Flag M2 affinity resin (Sigma) as described above and probed for Pin1 and Flag-tagged SLBP by Western blotting.

For coimmunoprecipitation of translation initiation factors with SLBP, HEK293 cells were treated with control or Pin1 siRNAs and the cells harvested. The cells were lysed as described above and immunoprecipitated with SLBP antibody toward the C-terminal 13 amino acids of human SLBP and probed for SLBP, eIF4G, and eIF4E by Western blotting.

Analysis of histone mRNA decay rates. HEK293 cells were synchronized by double thymidine block, released into S phase, and either mock treated with DMSO or treated with 20 μM PiB for a total of 16 h before being harvested. Actinomycin D was added to block transcription to a final concentration of 5 μg/ml to cells 6 h prior to harvesting. HEK293 cells (1×10^6) were harvested at different time points (0, 0.25, 0.5, 0.75, 1, and 1.25 h) after the addition of 5 mM hydroxyurea (HU) to trigger histone mRNA decay for analysis of mRNA levels. mRNA abundance was quantified using RT-PCR.

SLBP stability assay. HEK293 cells were mock treated with DMSO or treated with 20 μM PiB for 16 h. The levels of SLBP were analyzed at different time points (1, 2, 4, 6, and 8 h) after treatment with 50 μg/ml of cycloheximide (CHX) in the presence or absence of PiB.

Ubiquitination assays. HEK293 cells were transiently transfected with HA-ubiquitin and the Flag-tagged SLBP constructs with Lipofectamine 2000 (Invitrogen). Twenty-four hours later, the cells were treated with 20 μM PiB for 16 h or mock treated with DMSO as indicated below. The cells were treated with ALLN to inhibit the proteasome to a final concentration of 40 μM for 4 h prior to being harvested. After lysis with RIPA buffer (1% Nonidet P-40, 0.5% Triton X-100, 0.1% SDS, 50 mM Tris-HCl [pH 7.5], 150 mM NaCl, 0.5 mM EDTA, 25 μM ALLN, and protease inhibitors), protein extracts were incubated with anti-Flag beads (Sigma), washed five times, resolved by SDS-PAGE, and analyzed by Western blotting. In an alternative approach, Pin1 was knocked down by siRNA in HEK293 cells, and 48 h after the second hit, the cells were transiently transfected with $(His)_6$-ubiquitin and the Flag-tagged SLBP constructs. Twenty-four hours after transient transfection, the cells were blocked with ALLN. The control and siRNA-treated cells were lysed in 6 M guanidine HCl in PBS buffer (pH 8.5). The lysates were incubated with nickel affinity resin (Qiagen) with gentle agitation for 6 h to bind ubiquitinated proteins. The beads were washed sequentially with 6 M guanidine HCl at pH 8.5, 6 M guanidine HCl at pH 6.0, 6 M guanidine HCl at pH 7.0 with 10 mM imidazole, 6 M guanidine HCl at pH 7.0, 0.2% NP-40, and 20% glycerol in PBS. The bound proteins were eluted with 100 mM imidazole in PBS and were analyzed by Western blotting for SLBP and ubiquitin.

Mass spectrometry. (i) Sample preparation. HEK293 cells were transiently transfected with Flag-tagged wild-type SLBP using Lipofectamine 2000 for 24 h and then either mock treated with DMSO or treated with 20 μM PiB for 16 h. The cells were lysed and the lysates bound to anti-Flag M2 affinity gel (Sigma) by nutation with the beads for 12 h. The resin was washed three times with lysis buffer. Flag-tagged SLBP bound to the beads was eluted with 3× Flag peptide (Sigma). The control and PiB-treated eluates were dialyzed extensively in 0.1% acetic acid. For in-solution protein digestion, the samples were dried and dissolved in 8 M urea and 0.4 M ammonium bicarbonate (pH 8.0). The proteins were reduced by the addition of dithiothreitol (DTT) and then alkylated with iodoacetamide (IAN) by incubation in the dark for 20 min. Samples were then digested with trypsin at a 1:10 molar ratio of trypsin to SLBP by incubation at 37°C for 16 h.

For preparation for the liquid chromatography-tandom mass spectrometry (LC MS-MS) analysis, the phosphopeptides present in the tryptic digests were enriched using an in-house titanium oxide enrichment method. Briefly, the samples were acidified with 0.5% trifluoroacetic acid (TFA)–50% acetonitrile and loaded onto TopTips (Glygen Corp.), followed by washing three times with 100% acetonitrile, 0.2 M sodium phosphate buffer (pH 7.0), 0.5% TFA, and then 50% acetonitrile. Phosphopeptides were eluted from the TopTip using 28% ammonium hydroxide, dried in a SpeedVac, and then redried from water. Samples were resuspended in 70% formic acid and then immediately diluted out to 0.1% TFA for mass spectrometry analysis. The flowthrough from the washes and the enriched fractions were analyzed by LC MS-MS.

(ii) Data analysis and processing. Samples were analyzed by LC MS-MS using an LTQ Orbitrap Elite equipped with a Waters nanoAcquity ultraperformance liquid chromatography (UPLC) system using a Waters Symmetry C_{18} 180-μm by 20-mm trap column and a 1.7-μm (75-μm-inner-diameter by 250-mm) nanoAcquity UPLC column (35°C) for peptide separation. Trapping was done at 15 μl/min with

99% buffer A (100% water, 0.1% formic acid) for 1 min. Peptide separation was performed at 300 nl/min with buffer A and buffer B (100% CH_3CN containing 0.1% formic acid). A linear gradient (51 min) was run with 5% buffer B at initial conditions, 50% buffer B at 50 min, and 85% buffer B at 51 min. Mass spectral data were acquired in the Orbitrap using 1 microscan and a maximum inject time of 900 μs followed by data-dependent MS-MS acquisitions in the ion trap (via collision-induced dissociation [CID]) and in the high-energy collision dissociation (HCD) cell. Neutral loss scans (MS^3) were also obtained for 98.0, 49.0, and 32.7 atomic mass units (amu). The data were searched using Mascot Distiller and the Mascot search algorithm. The data were processed with Progenesis LCMS (Nonlinear Dynamics, LLC), and protein identification was performed using the Mascot search algorithm (Matrix Science).

For quantification of the relative enrichment of phosphopeptides, the control run was chosen as a reference, and the experimental run (+PiB) was chromatographically aligned to that run in order to minimize retention time variability between the two runs. No adjustments are necessary in the *m/z* dimension due to the high mass accuracy of the spectrometer (typically <3 ppm). Peak detection was set with default parameters (standard deviation of signal/noise of 3). A total of ~5,000 features were detected within retention time ranges of 16 to 100 min, for peptides having 7+ or fewer charges on them. A normalization factor (a global scaling factor) was calculated for each run to account for differences in sample loading between injections and minimum influence of noise in the data. The features (picked peaks) and their corresponding data-dependent MS-MS data were filtered to exclude spectra with a rank of >10 (only the top 10 MS-MS acquisitions per feature were included) or isotope of >3 to ensure that the highest-quality MS-MS spectral data were utilized for peptide assignments and subsequent protein identification (ID). The MS-MS data were exported to an .mgf (Mascot generic file) for database searching utilizing an in-house Mascot algorithm (version 2.2.0) (16) for uninterpreted MS-MS spectra after using the Mascot Distiller program to generate Mascot-compatible files. The Mascot Distiller program combines sequential MS-MS scans from profile data that have the same precursor ion. The Mascot search parameters utilized were partial methionine oxidation and carboxamidomethylated cysteine, a peptide tolerance of ±15 ppm, MS-MS fragment tolerance of ±0.6 Da, peptide charges of 7+ or fewer, and missed cleavages of 3 or fewer. Normal and decoy Swiss-Prot protein database searches were run, with GluC and trypsin as the enzymes used. The Mascot significance score match is based on a MOWSE (molecular weight search) score and relied on multiple matches to more than one peptide from the same protein. After the Mascot search, an .xml file of the results is created and then imported into the Progenesis LCMS software, where search hits are paired with the LCMS quantitation on the peptide mass.

Electrophoretic mobility shift assays (EMSA). Baculovirus-expressed human SLBP was incubated with a stem-loop probe labeled at the 5′ end with γ-^{32}P for 10 to 20 min on ice in binding buffer (20 mM Tris [pH 7.9], 20% glycerol, 100 mM KCl, 0.2 mM EDTA, 0.5 mM DTT, 0.1 mg/ml bovine serum albumin [BSA]). This preformed end-labeled stem-loop SLBP complex was then treated with Pin1 in either the presence or absence of the phosphatases PP2A and PP1. A 10-fold molar excess of cold competitor RNA was added to reaction mixtures after the preincubation period as specified below. All reaction mixtures were kept on ice for 5 min, after which they were run on a native gel to monitor dissociation of the complex. The total reaction volume (10 μl) was analyzed on an 8% native polyacrylamide Tris-borate gel run in Tris-borate buffer at 150 V for 1 to 1.5 h. The gel was dried at 80°C for 2 h and then exposed to film. All reactions were repeated 5 times, and the observed dissociation of the SLBP-RNA complex was reproducible with different stocks of human full-length SLBP and *Drosophila* full-length SLBP as well as the RBDs. The relative ratios of SLBP to Pin1 used are indicated in the figures and figure legends.

Fluorescence measurements to monitor Pin1-mediated dissociation of the SLBP-histone mRNA stem-loop complex. Fluorescence anisotropy measurements were performed with a Jobin-Yvon Horiba Fluoromax spectrofluorometer with a 26-nucleotide histone mRNA that was 3′end labeled with fluorescein in phosphate buffer. Unlabeled stem-loop RNA was used in the competition experiments. Proteins were titrated (as specified below) into a 0.5-cm quartz cuvette that contained the fluorescently labeled RNA solution, and the anisotropy was measured ($\lambda_{excitation}$ = 492 nm; $\lambda_{emission}$ = 518 nm) at 25°C. The data were fit in GraphPad Prism to the appropriate binding equations.

Fluorescence microscopy. HeLa cells grown on coverslips were washed with PBS and fixed in 4% formaldehyde in PBS for 15 min at room temperature. Cells were washed again and permeabilized in 0.5% Triton X-100 in PBS for 20 min. The cells were blocked with Image-iT FX signal enhancer (Invitrogen) for 30 min. The blocking solution was removed and the cells were washed once in PBS. Cells were incubated overnight with anti-HA antibody in 3% BSA–0.1% Triton X-100 in PBS. Coverslips were washed three times for 10 min each with 0.1% Triton X-100 in PBS. The cells were then incubated with Alexa Fluor 647 goat anti-mouse secondary antibody (Invitrogen) in 0.1% Triton X-100 in PBS for 1 h. Coverslips were 4′,6-diamidino-2-phenylindole (DAPI) stained and washed three times for 10 min each with 0.1% Triton X-100 in PBS. The coverslips were mounted onto slides using ProLong Gold antifade reagent (Invitrogen). Images were acquired using a Leica (DMIRE2) confocal microscope and analyzed using Leica software, version 2.61 (Leica Microsystems, Heidelberg, Germany).

In another series of experiments, HeLa cells grown on coverslips were incubated with 5-ethynyl-2′-deoxyuridine (EdU) solution at 37°C for 30 min as per the manufacturer's instructions (Click-iT EdU imaging kits; Invitrogen). After incubation, the cells were washed with PBS and fixed in 4% formaldehyde in PBS for 15 min at room temperature. Cells were then washed again and permeabilized in 0.5% Triton X-100 in PBS for 20 min. The permeabilization buffer was removed, and cells were washed twice with 3% BSA in PBS. Coverslips were inverted onto a drop of reaction cocktail and prepared as per the manufacturer's instructions. The cells were then washed with 3% BSA in PBS and blocked with Image-iT FX signal enhancer for 30 min. The blocking solution was removed, and the cells were washed once in PBS. Cells were incubated overnight with anti-HA antibody in 3% BSA–0.1% Triton X-100 in PBS. Coverslips were washed three times for 10 min each with 0.1% Triton X-100 in PBS. The cells were then incubated with Alexa Fluor 594 goat anti-mouse secondary antibody (Invitrogen) diluted 1:1,000 in 0.1% Triton X-100 in PBS for 1 h. Coverslips were DAPI stained and washed three times for 10 min each with 0.1% Triton X-100 in PBS. The coverslips were mounted onto slides using ProLong Gold antifade reagent (Invitrogen). Immunofluorescence was detected with Chroma filter sets using an Olympus BX51 upright microscope (100× plan-apo, oil, 1.4 numerical aperture [NA]) equipped with a Sensicam QE (Cooke Corporation) digital charge-coupled device (CCD) camera, motorized Z-axis controller (Prior), and Slidebook 4.0 software (Intelligent Imaging Innovations, Denver, CO). Optical sections were collected at 0.5-mm intervals through the Z axis and processed using no-neighbor deconvolution (Slidebook 4.0).

NMR chemical shift mapping to study the SLBP-Pin1 interaction. NMR experiments were performed on an Inova 700-MHz spectrometer with cryoprobe at 298 K. The ^{15}N-Pin1 sample was buffer exchanged into 20 mM Tris acetate buffer, 50 mM NaCl (pH 6.0), 50 mM sodium sulfate, 1 mM DTT, and 90% H_2O–10% ^2H_2O for NMR analysis. Phosphorylated or unphosphorylated SLBP peptides were taken up in the NMR buffer and were titrated into a 0.25 mM uniformly ^{15}N-labeled Pin1 NMR sample up to a 1:10 (Pin1/peptide) molar ratio. The spectral changes were monitored by acquiring a series of sensitivity-enhanced (^{1}H, ^{15}N) heteronuclear single quantum coherences (HSQCs) at peptide/Pin1 molar ratios of 0.1, 0.2, 0.3, 0.4, 0.5, 0.75, 1.0, 3.0, 5.0, and 10.0. ^{1}H and ^{15}N chemical shift assignments of Pin1 were obtained from the BioMagResBank (BMRB) (ID number 5305). Pin1 amide resonances were in either fast or intermediate

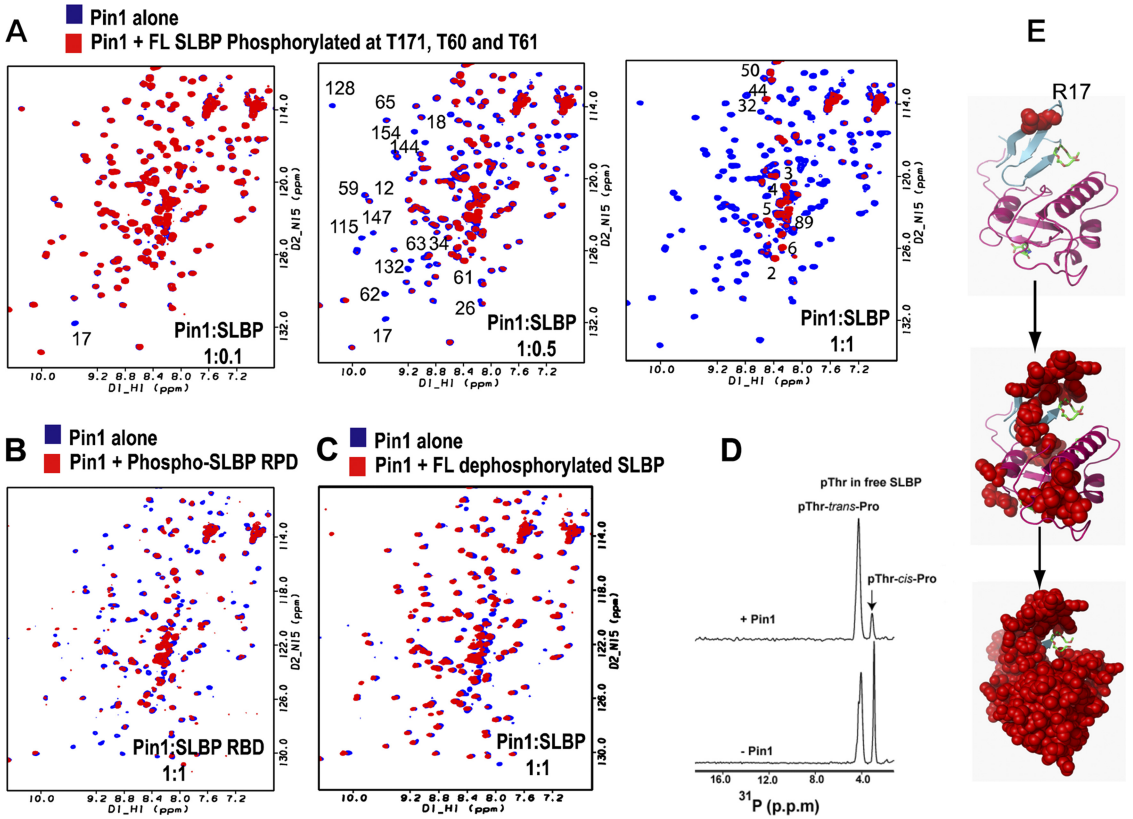

FIG 1 Phosphorylated SLBP forms a specific complex with the prolyl isomerase Pin1 *in vitro*. (A) Chemical shift mapping of uniformly ^{15}N-labeled Pin1 was performed with the addition of increasing concentrations of unlabeled phosphorylated full-length SLBP. ^{15}N-labeled Pin1 (0.25 mM) was titrated with increasing molar ratios of phosphorylated SLBP (phospho-SLBP) as indicated. The free (^{1}H, ^{15}N) HSQC Pin1 spectrum is shown in blue, and the (^{1}H, ^{15}N) HSQC Pin1 spectrum with SLBP is shown in red. All spectra were apodized identically and are plotted at the same contour level. At a substoichiometric ratio of 0.5:1 for phospho-SLBP to Pin1, several Pin1 amides in the WW domain and the catalytic domain that are known to be part of ligand binding sites disappear from the spectrum. These residues have been mapped onto the crystal structure of Pin1 (pdb code 1PIN in panel E). Only resonances from the disordered N terminus remain visible (residue numbers are indicated) in the spectrum in the presence of an equivalent amount of phospho-SLBP. For panel B, a similar titration was performed with baculovirus-expressed hSLBP RPD. The overlay of the free and RPD-bound Pin1 spectra is shown (C). No perturbations were observed in the Pin1 spectrum when dephosphorylated SLBP (baculovirus expressed and treated with calf intestinal phosphatase) was titrated into the spectrum. (D) ^{31}P NMR spectra of phosphorylated human SLBP RPD are shown in the presence and absence of Pin1. Two resonances for a single phosphate on Thr171 are observed in the 1D ^{31}P spectrum due to *cis-trans* isomerization about the Thr-Pro bond. Addition of Pin1 changes the populations of the two conformers. (E) The chemical shift perturbations from the NMR titration are depicted in red on the crystal structure of Pin1 (PDB code 1PIN).

exchange during the course of the NMR titration. No chemical shift perturbations occurred in the presence of the unphosphorylated peptide control. For resonances that exhibited fast-exchange behavior as a result of added peptide, the total chemical shift perturbation (^{1}H + ^{15}N) in hertz was plotted against the ratio of peptide to Pin1. The fractional change in chemical shift is related to the dissociation constant via the following relationship: $\Delta\delta = [(\delta_b - \delta_f)/2][1 + (pep_o/P_o) + 1 - Sqrt(1 + pep_o/P_o + K_d/P_o)2 - 4pep_o/P_o]$, where $\Delta\delta$ is the observed chemical shift, δ_f is the chemical shift of free Pin1, δ_b is the chemical shift of fully bound Pin1, pep_o is the total peptide concentration, and P_o is the total Pin1 concentration. Values for dissociation constant (K_d) and the difference between δ_b and δ_f were obtained by simultaneous fitting of the observed perturbations for five residues to the above equation using a least-squares fit and assuming a single binding site model. ^{1}H and ^{15}N chemical shift assignments of Pin1 were obtained from the BMRB (ID number 5305).

RESULTS

Structural basis for the phosphorylated SLBP-Pin1 interaction. We used an NMR-based chemical shift mapping assay to investigate (i) whether Pin1 directly binds SLBP and (ii) if the interaction is specific for phosphorylated SLBP. Since the interaction of Pin1 with its substrates has been well characterized by NMR (13, 19, 26–28, 43) and X-ray crystallography (45, 54, 66), this approach allowed us to determine whether SLBP interacted with Pin1 in a specific manner. In this assay, phosphorylated SLBP at natural isotope abundance was titrated into a solution of "NMR active" ^{15}N-labeled Pin1, and the spectral and conformational changes in Pin1 were monitored in the presence of increasing amounts of unlabeled full-length phosphorylated SLBP (P-SLBP) by collecting a series of (^{1}H, ^{15}N) HSQC spectra (Fig. 1A). Since the SLBP is not isotopically labeled, it is invisible during the titration. As the backbone amide resonances of Pin1 are assigned, this approach gives site-specific information about which amides are sensitive to the presence of the SLBP ligand. The changes in the NMR spectra can be mapped onto the structure of Pin1 to determine the binding interface (18, 19). Pin1 has a two-domain structure (45) consisting of an N-terminal WW domain that specifically recognizes phosphorylated Ser/Thr-Pro sequences and a catalytic PPIase domain (Fig. 1). Two side chains on Pin1 make specific contacts with the substrate in Pin1-substrate crystal struc-

tures (45, 54): Trp34 in the WW domain of Pin1 stacks with the substrate proline, while Arg17 interacts with the substrate phosphates. The complex was in intermediate exchange, and a number of resonances broadened out of the Pin1 spectrum in the presence of P-SLBP. The first residue to disappear from the spectrum at a molar ratio of P-SLBP to Pin1 of 0.1:1 was Arg17 in the WW domain of Pin1. An increase in the concentration of P-SLBP resulted in disappearance of additional residues around Arg17 in the WW domain. Consistent with previous analysis of Pin1-substrate interactions, spectral perturbations were found to propagate from the WW domain toward the PPIase domain in response to P-SLBP. At a substoichiometric ratio of 0.5:1 for P-SLBP to Pin1, several Pin1 amides in the WW domain and the catalytic domain disappear from the spectrum (Glu12, Arg14, Ser18, Phe25, Asn26, Ile29, Asn30, Gln33, Trp34, Ser58, His59, Leu61, Val62, Lys63, Ser65, Ile78, Thr79, Thr81, Ser115, Gly120, Leu122, Gly128, Gln129, Lys132, Ser138, Gly144, Ser147, Gly148, Thr152, Ser154, Ile158, Ile159, and Arg161). These residues have been mapped onto the crystal structure of Pin1 (Fig. 1E). At a stoichiometric ratio of P-SLBP to Pin1, almost all Pin1 resonances broaden out of the spectrum, with the exception of residues from the flexible N terminus. No spectral changes are observed in the presence of dephosphorylated SLBP (Fig. 1C). Therefore, the pattern of chemical shift broadening observed indicates that Pin1 forms a specific complex with full-length phosphorylated SLBP *in vitro*. Using GST-Pin1 as bait, we were also able to pull out HA-SLBP from HeLa cells that stably expressed HA-SLBP. HA-SLBP was identified by Western blotting as well as MALDI-time of flight (TOF) mass spectrometry to be hSLBP (data not shown).

We also compared the binding of different SLBP phosphopeptides comprising the SFTTP sequence in the SLBP N terminus and the HPKTPNK sequence in the RNA binding domain (see Fig. S1 in the supplemental material) to ^{15}N-labeled Pin1 using NMR chemical shift mapping experiments as described above for full-length phosphorylated SLBP. The phosphorylated peptides bound Pin1 less tightly than the full-length phosphorylated protein, with both peptides binding Pin1 with a K_d of ~1 μM as was estimated from NMR titrations. Under saturating conditions, where the peptide/Pin1 molar ratio is 10:1, all peptides showed very similar chemical shift perturbations of Pin1 amides. No perturbations in the Pin1 spectrum were observed for the unphosphorylated peptides.

Since the SLBP RPD exhibits proline isomerization about the phosphor-Thr171-Pro172 bond, we also titrated baculovirus-expressed SLBP RPD into a solution of ^{15}N-labeled Pin1 (Fig. 1B). The baculovirus-expressed SLBP RPD was phosphorylated only on one site (3), as we confirmed by electrospray ionization mass spectrometry, and phosphorylation at this site appears to be stoichiometric (3). We have no evidence for the presence of unphosphorylated SLBP RPD by either mass spectrometry or gel filtration (65). Titration of an equimolar equivalent of SLBP RPD (1:1) into a solution of ^{15}N-labeled Pin1 resulted in broadening of cross-peaks corresponding to residues in both the WW domain and the prolyl isomerase domain of Pin1 in the (^{1}H, ^{15}N) HSQC spectrum of Pin1, in a manner similar to that observed for the full-length SLBP. Therefore, the isolated SLBP RPD forms a specific complex with Pin1. To determine whether Pin1 also isomerized the SLBP RPD about the Thr-Pro bond in the TPNK sequence, we collected 1D ^{31}P NMR spectra (Fig. 1D) for the SLBP RPD at pH 8.0 in the presence and absence of Pin1. We have recently shown (65) that human and *Drosophila* SLBP RPDs are unstable and that the ^{1}H NMR spectra are not tractable to analysis by NMR. This prevents application of traditional exchange spectroscopy NMR experiments to study proline isomerization in the intact SLBP RPD. The instability of the SLBP RPD is in large part due to proline isomerization about the Thr171-Pro172 sequence. However, the ^{31}P NMR spectra of baculovirus-expressed SLBP RPD that is phosphorylated only at Thr171 in human SLBP show two resonances for a single phosphate in the RBD at basic pH due to *cis-trans* proline isomerization (Fig. 1D). Addition of Pin1 changes the relative populations of the *cis* and *trans* conformers in the ^{31}P spectra, confirming that Pin1 not only binds but also isomerizes SLBP in the RPD (Fig. 1D).

Pin1 dissociates SLBP from the histone mRNA stem-loop. Next, we investigated whether addition of Pin1 affected the stability of the SLBP-histone mRNA complex by EMSA and fluorescence anisotropy assays (Fig. 2). We used full-length phosphorylated *Drosophila* SLBP (dSLBP), hSLBP, and hSLBP RBD expressed in baculovirus for this analysis. dSLBP is phosphorylated predominantly in the RPD (7), and one additional phosphorylation site in the N terminus at T120 is present (29). In contrast, baculovirus-expressed full-length hSLBP is a heterogeneous mixture of at least 23 different phosphorylation sites (Lam and Thapar, unpublished), but it is stoichiometrically phosphorylated at T171 in the RBD. The hSLBP RBD is phosphorylated only on T171. A preformed complex of phosphorylated dSLBP and stem-loop RNA labeled at the 5′ end with γ-^{32}P was treated with Pin1 in the presence and absence of cold competitor RNA, and EMSAs were performed (Fig. 2A). When the 5′-end-labeled RNA probe is mixed with SLBP and run on a native gel, the protein-RNA complex mobility is retarded, as is expected for a stable complex (Fig. 2A to C). The cold RNA competitor was added 20 min after the 5′-end-labeled stem-loop RNA was incubated with SLBP. Addition of a 10-fold excess of cold competitor RNA to the preformed complex does not result in dissociation of the complex as shown in Fig. 2B. When increasing amounts of Pin1 are added to the reaction in the absence of cold RNA, a slight retardation in the mobility is observed (Fig. 2A, left), indicating that Pin1 may form a ternary complex with the SLBP and histone mRNA. However, addition of a 10-fold excess of cold competitor RNA in the presence of Pin1 results in complex dissociation and partial exchange of the labeled and unlabeled RNA. The radioactive free probe is released and runs at the bottom of the gel (Fig. 2A, middle). Increasing the concentration of Pin1 results in a corresponding increase in the release of the free probe, indicating that the effect is directly due to Pin1 activity (Fig. 2A, middle). Pin1 is also known to interact with PP2A *in vivo* to dephosphorylate Pin1 targets. Interestingly, when PP2A is added to the preformed complex of SLBP and 5′-end-labeled RNA complex (in the absence of Pin1), the complex is highly stable and does not dissociate even when a 10-fold excess of cold RNA is present in the reaction, as probed by EMSA (Fig. 2B, lanes 1 and 2). However, when catalytic amounts of PP2A are added along with Pin1 and an excess of cold competitor RNA, free ^{32}P-labeled stem-loop RNA is observed at the bottom of the gel (Fig. 2A, right). As previously shown, the unphosphorylated SLBP has a high off-rate, allowing exchange of the labeled and unlabeled RNA (65). Increasing the concentration of Pin1 facilitates dissociation in the presence of PP2A. Therefore, a Pin1-mediated conformational change is required to facilitate

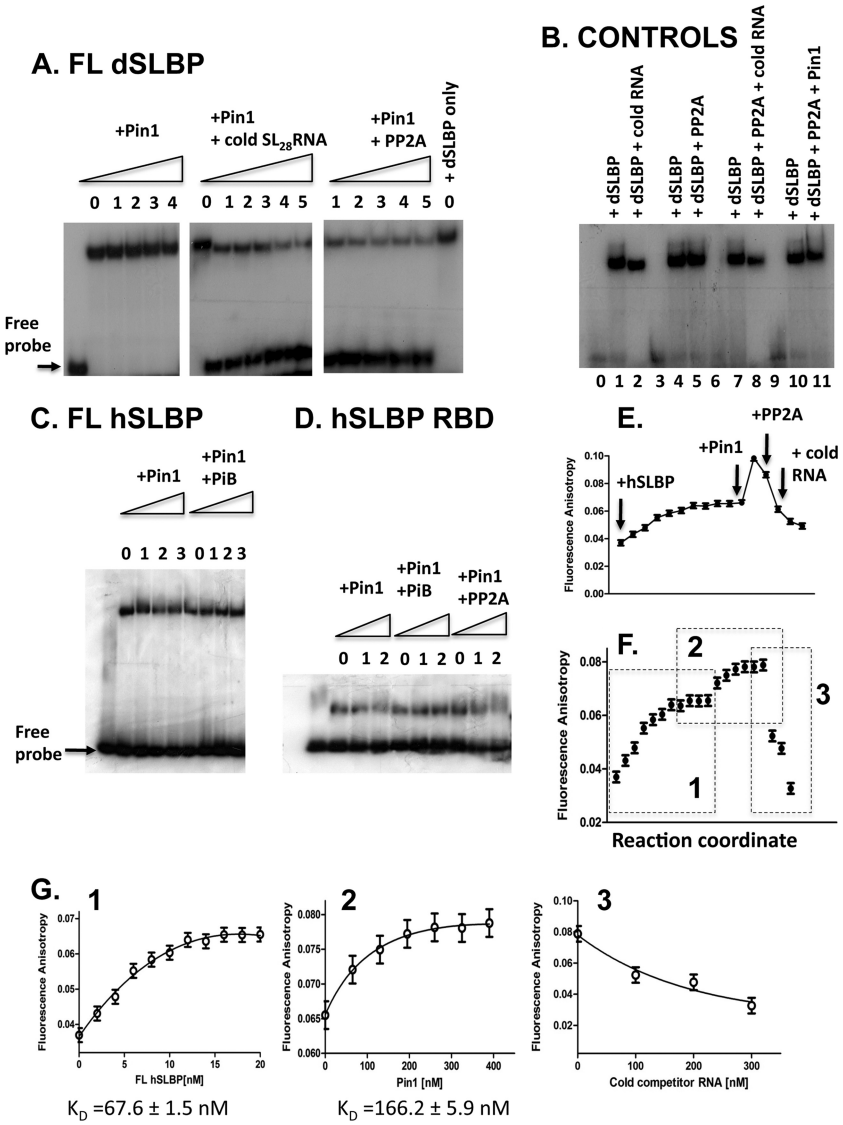

FIG 2 The SLBP-histone mRNA complex dissociates in the presence of Pin1 and PP2A. (A) Dissociation of the dSLBP-RNA complex monitored by EMSA. ^{32}P-labeled histone stem-loop RNA was incubated with the baculovirus-expressed full-length (FL) dSLBP on ice either with or without the various enzymes as indicated. (Left) Addition of Pin1 alone does not dissociate the preformed dSLBP-RNA complex. SLBP was at 40 nmol in all lanes in a total reaction volume of 10 μl, whereas the Pin1 concentrations were 50 nmol (lane 1), 100 nmol (lane 2), 200 nmol (lane 3), and 400 nmol (lane 4). No Pin1 was added to the "0" lane. The ^{32}P-labeled RNA was at 1 pmol in all lanes. (Middle) Addition of increasing concentration of Pin1 and a 10-fold excess of SL_{28} RNA (relative to the ^{32}P-labeled RNA) results in accumulation of free [^{32}P]ATP at the bottom of the gel. SLBP was at 40 nmol in all lanes in a total reaction volume of 10 μl, whereas the Pin1 concentrations were 50 nmol (lane 1), 100 nmol (lane 2), 200 nmol (lane 3), 400 nmol (lane 4), and 800 nmol (lane 5). No Pin1 was added to the "0" lane. (Right) The ^{32}P-labeled histone stem-loop probe is released more efficiently when the complex is incubated with increasing concentrations of Pin1 and a fixed concentration (0.3 nmol) of PP2A. The concentrations of SLBP, RNA, and Pin1 are the same as those described for the middle panel. (B) The control panel shows that addition of neither cold RNA alone nor phosphatase alone results in dissociation. Dissociation is observed only when Pin1 is present in the presence of excess competitor RNA. (C) Binding of Pin1 to the full-length baculovirus-expressed phosphorylated human SLBP-RNA complex was monitored by EMSA in the presence and absence of the Pin1 inhibitor PiB, but without excess competitor RNA. No effect of Pin1 was apparent on the preformed complex in either reaction. (D) Binding of Pin1 of the baculovirus-expressed phosphorylated human SLBP-RPD RNA complex was monitored by EMSA in the presence and absence of the Pin1 inhibitor PiB and PP2A. Addition of Pin1 and PP2A to the human SLBP RPD-RNA complex (in the absence of competitor RNA) results in the complex running diffuse through the gel, indicating that some dissociation occurs even in the absence of cold RNA. The SLBP RBD was at 10 nmol, the ^{32}P-labeled RNA was at 0.5 pmol, Pin1 was at 20 nmol (lane 1) and 40 nmol (lane 2), and PP2A was at 0.3 nmol. (D) Fluorescence anisotropy for the association of 3′ fluorescein-labeled histone stem-loop RNA with phosphorylated full-length human SLBP, Pin1, PP2A, and a 10-fold excess of unlabeled competitor RNA is shown. Addition of Pin1 to the SL28-SLBP binary complex results in an increase in fluorescence anisotropy. Addition of PP2A results in a small decrease in the anisotropy, and a complete decrease in anisotropy to baseline is observed when unlabeled SL_{28} RNA is added to the (SL_{28} plus hSLBP-Pin1 plus PP2A) mixture. (E) Binding isotherm for interaction of human SLBP with 3′ fluorescein-labeled histone stem-loop RNA (1), addition of Pin1 to the SLBP-RNA complex in the absence of competitor RNA (2), and addition of Pin1 and PP2A to the SLBP-RNA complex in the presence of competitor RNA (3) is shown. In panel F, the individual isotherms for these reactions are shown. The apparent dissociation constants derived from the observed change in anisotropy are indicated. The concentration of RNA for the fluorescence experiments was 50 nM, and 0.02 μg of a 0.1 mg/ml solution of PP2A (corresponding to 0.4 enzyme units) was added to the 500-μl reaction mixture. (G) The concentrations of hSLBP and Pin1 are indicated. All fluorescence experiments were performed at 25°C in PBS buffer (pH 7.4), and each data point was measured in triplicate.

phosphatase activity. No dissociation is evident in the absence of cold competitor RNA or with PP2A alone (Fig. 2B).

To confirm the results of the EMSAs, we used fluorescence anisotropy to characterize the SLBP-RNA binding reactions in the presence of Pin1 and/or PP2A. The histone mRNA stem-loop was labeled at either the 5′ or 3′ end with fluorescein (FAM), and the binding of human SLBP to labeled RNA was characterized in the presence and absence of Pin1 and the phosphatases by fluorescence anisotropy. Introduction of 5′ FAM was detrimental to complex formation (data not shown). This is likely due to steric effects, since the 5′ flanking region is important for SLBP-RNA contacts (59). Therefore, all binding experiments were performed with histone mRNA stem-loop with 3′-end FAM. Addition of phosphorylated full-length baculovirus-expressed SLBP to histone stem-loop labeled with fluorescein at the 3′ end results in an increase in anisotropy due to formation of the SLBP-RNA complex (Fig. 2E). When fit to a 1:1 binding isotherm, the results yield a K_d of 67.6 ± 1.5 nM (Fig. 2E to G). When Pin1 is titrated into this complex (in the absence of unlabeled competitor RNA), a steady increase in fluorescence anisotropy is observed, as indicated by the EMSA indicating formation of a ternary (Pin1-SLBP-RNA) complex. The apparent K_d for Pin1 interaction with the SLBP-RNA complex was determined to be 166.2 ± 5.9 nM (Fig. 2E to G). When PP2A is added to the Pin1-SLBP-RNA complex, a small but significant decrease in fluorescence anisotropy is observed (Fig. 2E), indicating that PP2A promotes dissociation of the complex, but in the absence of cold competitor RNA there is probably rebinding of SLBP to the labeled RNA. However, addition of a 10-fold excess of unlabeled stem-loop RNA to this mixture containing Pin1 and PP2A competes off SLBP from the fluorescein-labeled RNA, and the anisotropy value returns to that of the free fluorescein-labeled RNA at the beginning of the titration (Fig. 2E to G). Thus, the fluorescence anisotropy and the mobility shift assays suggest that Pin1 and a phosphatase such as PP2A can act to increase the off-rate of SLBP from the stem-loop at the 3′ end of histone mRNA, allowing exchange of labeled and unlabeled RNA in the complex. The results are consistent with our published studies (3, 65) showing that SLBP that is dephosphorylated at Thr171 has a higher off-rate for the histone mRNA stem-loop.

The requirement for both Pin1 and PP2A to dissociate a highly specific and stable SLBP-RNA complex is an unexpected result but of great potential significance. It suggests that the enzymes might work together in the cell to dissociate SLBP from the histone mRNA or pre-mRNA. Since the catalytic synergy between Pin1 and PP2A has also previously been reported for the Pin1 substrates Cdc25 (68) and Raf-1 (8), a likely candidate for the phosphatase that dephosphorylates SLBP *in vivo* is PP2A.

Pin1 regulates SLBP protein stability and its ubiquitination. In order to determine the effects of Pin1 isomerase activity on SLBP levels, we knocked down Pin1 in HeLa cells (Fig. 3A) and HEK293 cells (Fig. 3B) using either a pool of four different siRNAs or a single siRNA. HeLa cells were transfected with either S2 or control (C2) siRNA against Pin1. These S2 siRNAs were specific for Pin1, since similar biological effects were observed irrespective of the siRNA used and independent of the cell line, suggesting that off-target effects were minimal. Pin1 siRNA knockdown had no effect on the protein levels of actin and several other proteins tested, including factors necessary for 3′-end cleavage and polyadenylation, such as CPSF73, CPSF100, and symplekin, that are required for processing of both poly(A)$^+$ and histone mRNAs (Fig. 3A; see also Fig. S2 in the supplemental material). These factors were all unaffected by Pin1 knockdown with the exception of CPSF160, which increased after Pin1 knockdown. CPSF160 is the RNA binding protein component of the cleavage and polyadenylation complex (CPSF) that may participate in processing both polyadenylated and histone mRNAs (22). Pin1 protein levels did not change appreciably in the presence of the C2 control during 72 h (Fig. 3A). Intriguingly, we found time-dependent accumulation of SLBP in HeLa cells as well as HEK293 cells that were treated with Pin1 siRNA, but not in those treated with the C2 siRNA. The increased protein levels of SLBP after siRNA knockdown could be rescued within 24 h after transfection of exogenous Flag-tagged Pin1 (Fig. 3D). In addition to SLBP, we tested the levels of other polyadenylation factors such as CPSF73, CPSF100, and symplekin that are required for processing of both poly(A) and histone mRNAs. These factors were all unaffected by Pin1 knockdown, with the exception of CPSF160, which increased after Pin1 knockdown (see Fig. S2 in the supplemental material).

Pin1 has been shown to be a mitotic regulator (37), and Pin1 knockdown in mouse embryonic fibroblasts (MEFs) (63) has previously been reported to show increased accumulation of cells in G_1 phase and decrease in G_2/M cells due to slower cell cycle progression, inability of cells to synthesize DNA, and deregulation of cyclin E, a target of Pin1. To see whether we observed a similar effect in HeLa cells, we performed fluorescence-activated cell sorting (FACS) on our S2- and C2-treated samples (Fig. 3E). Similar to the previous study, we observed an accumulation of cells in G_1 and a decrease in S-phase and G_2/M-phase cells, suggesting that an ~75% knockdown of Pin1 slowed progression to S phase. FACS analysis on HeLa cells (Fig. 3E) showed that after Pin1 knockdown in HeLa cells, there were significantly fewer cells in S phase (18%) as well as G_2 (6.5%) among Pin1 knockdown cells than among those treated with the C2 siRNA (26.5% in S; 12% in G_2), suggesting that Pin1 knockdown slowed cell cycle progression into S phase. Since SLBP is expressed only during S phase (58), the increase in accumulation of SLBP that is observed in Pin1 siRNA-treated cells is likely underestimated, as there are ~30% fewer cells in S phase among these cells.

To confirm that the observed increase in SLBP levels could be attributed to Pin1 activity, we analyzed SLBP levels after treating HEK293 cells with the Pin1 inhibitor PiB (Fig. 3C). PiB is highly selective toward Pin1 and inhibits Pin1 isomerase activity (53). A similar increase in SLBP levels was observed after chemical inhibition of Pin1 (Fig. 3C and F), indicating that Pin1 regulated SLBP levels. The mRNA levels of SLBP were also probed in PiB-treated cells by reverse transcription-PCR (Fig. 3C) and they remained identical to those of the control. The effect of PiB on SLBP stability was measured in HEK293 cells in the presence and absence of PiB by treating cells with cycloheximide and monitoring the decrease in SLBP levels over time (Fig. 3F). There was a clear difference in the rate of decay of SLBP particularly during the first 4 h after treatment with cycloheximide, indicating that Pin1 increased SLBP stability.

To determine whether Pin1 interacted directly with SLBP *in vivo*, HeLa cell lysates were treated with an anti-Pin1 antibody and the immunoprecipitates were analyzed for SLBP and Pin1. We also did the reciprocal experiment using SLBP antibody and observed very efficient coimmunoprecipitation of the two proteins

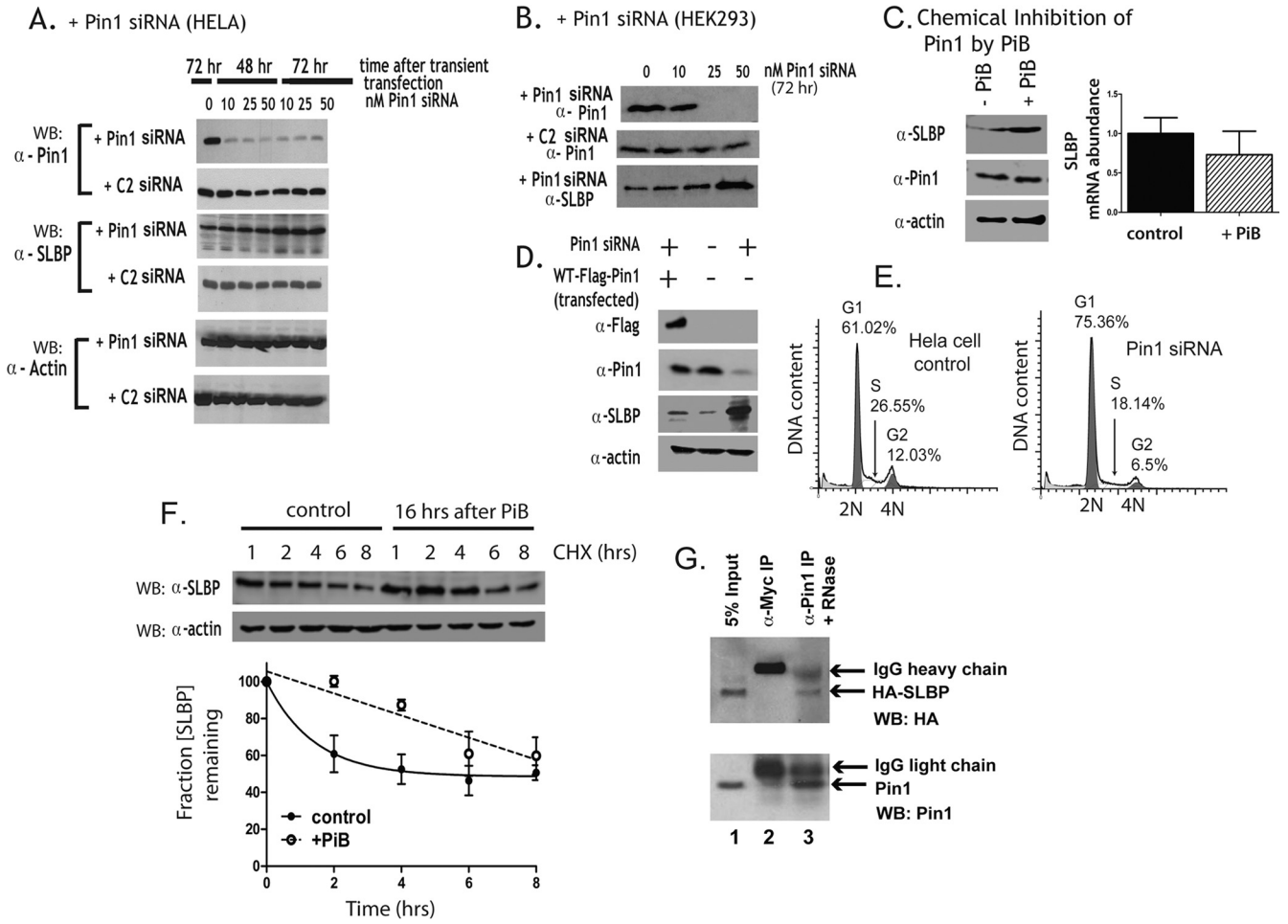

FIG 3 Pin1 inhibition increases SLBP levels. (A) HeLa cells were treated with either S2 or C2 siRNA for up to 72 h using a standard two-hit method. The levels of Pin1, SLBP, and actin were probed by Western blotting (WB) as noted. (B) HEK293 cells were treated with either S2 or C2 Pin1 siRNA for 72 h, and the cells were probed for Pin1 and SLBP. (C) Pin1 activity was inhibited by the addition of 20 μM PiB inhibitor for 16 h, whereas control cells were mock treated with DMSO. The protein levels of SLBP, Pin1, and actin were determined by Western blotting. The SLBP mRNA levels were also quantified in the control and PiB-treated cells by RT-PCR. (D) The effect of the Pin1 siRNA on SLBP levels could be rescued by the transfection of exogenous WT Flag-tagged Pin1 for 24 h into HEK293 cells after Pin1 was knocked down by 50 nM siRNA for 48 h. (E) Pin1 knockdown results in increased accumulation of cells in G_1 and reduced accumulation in S and G_2 phases. Cell cycle profiles of HeLa cells treated with either 25 nM Pin1 siRNA (S2) or 25 nM control RNA (C2) for 72 h were pulse-labeled with propidium iodide; the DNA content was analyzed by flow cytometry, and the cell cycle distribution was determined using the ModFit software. (F) The Pin1 inhibitor PiB affects the stability of SLBP. The levels of SLBP were analyzed at different time points after treatment with cycloheximide in the presence and absence of the Pin1 inhibitor PiB. The protein levels were quantified using ImageQuant software. (G) Pin1 coimmunoprecipitates with HA-SLBP. HeLa cell lysates were prepared from a cell line that stably expressed HA-SLBP. The lysates were treated with Pin1 antibody as described in Materials and Methods. Anti-Myc antibody was used as the control. The immunoprecipitates were run on SDS-PAGE and probed for Pin1 and HA-SLBP. A total of 5% of the input was run in the first lane as a control. No SLBP is observed in the anti-Myc control lane (lane 2).

(Fig. 3G). This interaction is not RNA dependent, since treatment of the lysates with RNase prior to immunoprecipitation did not abolish the interaction (Fig. 3G). Therefore, the two proteins interact directly *in vivo*.

There are six different Ser-Pro/Thr-Pro sites present in human SLBP, and previous phosphoproteomic analysis has shown that each of these sites is phosphorylated *in vivo* (12). Of these, two sites have been well characterized: one corresponding to the $SFT^{60}T^{61}P$ sequence in the SLBP N terminus (67) and the second corresponding to a conserved $T^{171}PNK$ sequence in the SLBP RNA binding domain that is important for RNA binding (29). To determine which phospho-Thr-Pro site was being targeted by Pin1 *in vivo*, we transiently transfected Flag-tagged wild-type SLBP into HEK293 cells and after 24 h either mock treated the cells with DMSO or treated them with the Pin1 inhibitor PiB. The Flag-tagged SLBP was purified using anti-Flag resin as described in Materials and Methods, and the highly purified protein was analyzed by mass spectrometry (Fig. 4). Several unique phosphopeptides were identified in human SLBP, and the data confirmed that human SLBP is phosphorylated at three additional Ser-Pro sites in the N terminus, namely, Ser7, Ser20, and Ser23 (Fig. 4). When the relative enrichment of phosphopeptides was quantified in PiB-treated cells relative to the control untreated cells by mass spectrometry, we observed 2- to 3-fold phosphate enrichment at Ser7, Ser20, Ser23, Ser221, Ser222, and Thr226 in addition to Thr171. The Thr171 site showed the largest change in relative enrichment. We did not observe phosphopeptides corresponding to Thr60 or Thr61 in the SFTTP sequence. These are likely of low

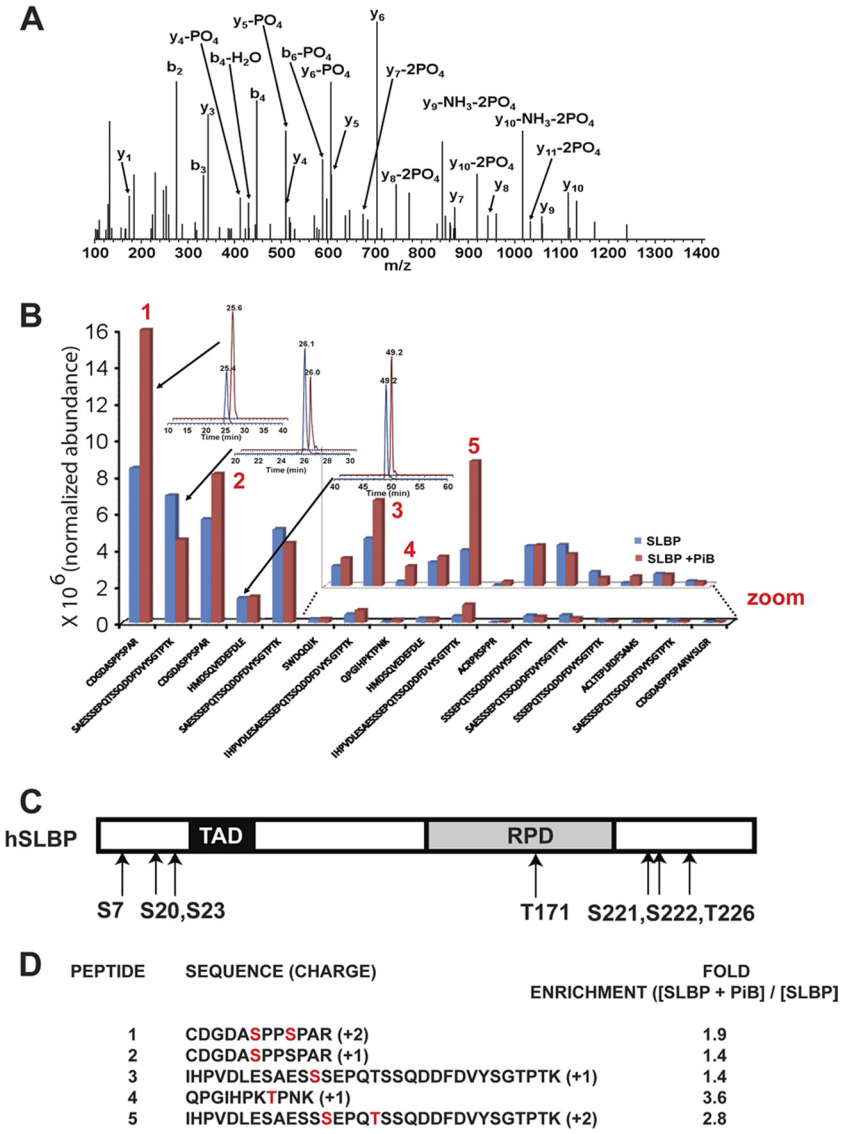

D

PEPTIDE	SEQUENCE (CHARGE)	FOLD ENRICHMENT ([SLBP + PiB] / [SLBP]
1	CDGDASPPSPAR (+2)	1.9
2	CDGDASPPSPAR (+1)	1.4
3	IHPVDLESAESSSEPQTSSQDDFDVYSGTPTK (+1)	1.4
4	QPGIHPKTPNK (+1)	3.6
5	IHPVDLESAESSSEPQTSSQDDFDVYSGTPTK (+2)	2.8

FIG 4 Identification of SLBP phosphorylation sites upregulated in response to PiB inhibitor by mass spectrometry. Several phosphorylation sites in human SLBP were mapped using high-resolution tandem mass spectrometry. The MS-MS spectrum in panel A illustrates a typical high-energy C-trap dissociation (HCD) fragmentation pattern obtained on an LTQ Orbitrap Elite MS instrument for an SLBP phosphorylated peptide (in this case, it is peptide 1 in panel D showing phosphorylation of S20 and S23). The bar graph in panel B compares the normalized abundance (based on a global scaling factor of all observable peptides in the LCMS experimental run) of SLBP phosphorylated peptides obtained from HEK293 cells treated without (blue) or with (red) 20 μM PiB inhibitor. Mass spectra were compared using Nonlinear Dynamics' Progenesis LCMS software (version 3.1.4003.30577) as described in Materials and Methods. The three inset chromatographs show the elution profiles of a phosphopeptide that was upregulated in the presence of PiB (top), a downregulated phosphopeptide (middle), and a phosphopeptide whose abundance was comparable (lower) in SLBP isolated in the presence or absence of PiB. The zoom in the inset illustrates additional phosphorylated SLPB peptides of lower abundance that show significant upregulation (labeled 1, 2, 3, 4, and 5) in the presence of PiB. (Note that the chromatographs corresponding to SLBP + PiB are offset.) (C) The domain organization of human SLBP is shown. TAD, translation activation domain; RPD, RNA binding and processing domain. Ser/Thr phosphorylation sites that show at least a 2-fold increase in abundance in the presence of PiB are shown. In panel D, the phosphorylated peptides identified are shown along with the corresponding fold enrichment in the presence of PiB. The numbering of the peptides corresponds to that depicted in panel B.

abundance, particularly in an asynchronous population of HEK293 cells, since T61 is phosphorylated by cyclin A/Cdk1, which is present at the end of S phase but not at other times during the cell cycle. The mass spectrometry data suggested that there are several phosphorylation sites that are targeted by Pin1 in human SLBP besides Thr171. We next transiently transfected the Flag-tagged SLBP WT and mutant proteins and pulled down the SLBPs using an anti-Flag resin. The resin was washed and then probed for the presence of Pin1 by Western blotting (Fig. 5E). We found that no single point mutant completely abolished interaction with Pin1; however, the SLBP Thr60A/Thr61A/Thr171A triple mutant showed a significant reduction in binding to Pin1. Therefore, in addition to Thr171 in the SLBP RPD, there are additional Ser/Thr-Pro sites in the SLBP N-terminal domain that are targeted by Pin1. Since there are two binding sites on Pin1 for phosphopeptides, one in the WW domain and the second in the prolyl isomerase

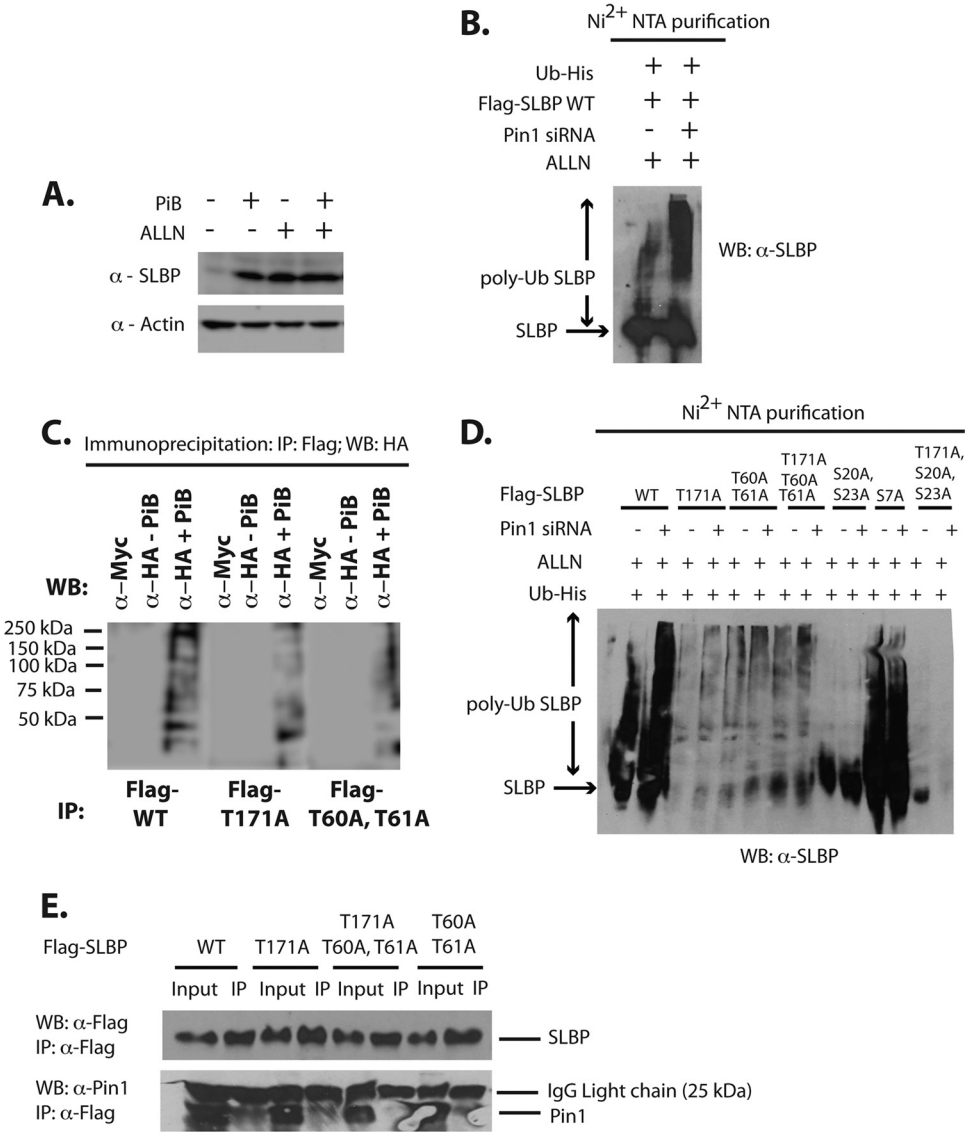

FIG 5 Pin1 regulates SLBP ubiquitination. (A) SLBP is degraded by the proteasome and Pin1. HEK293 cells were either treated with 20 μM PiB for 16 h or mock treated with DMSO to inhibit Pin1 as indicated, and/or treated with the proteasome inhibitor ALLN for 4 h before harvest. The SLBP and actin levels were probed in these cells by Western blotting. For panel B, HEK293 cells were treated with either control or Pin1 siRNA for 48 h, after which they were transiently cotransfected with $(His)_6$-tagged ubiquitin and Flag-tagged WT SLBP followed by treatment with ALLN. The lysates were purified on a nickel column as described in Materials and Methods to capture ubiquitinated proteins and then probed for ubiquitinated SLBP using an anti-SLBP antibody. (C) Flag-tagged SLBP WT or T171A or T60A/T61A mutants were immunoprecipitated (IP) from HEK293 cells expressing these proteins along with HA-tagged ubiquitin in the presence or absence of PiB inhibitor. Anti-Myc antibody was used as a control. The ubiquitinated SLBP was probed using the anti-HA antibody. (D) Pin1 siRNA increases accumulation of ubiquitinated SLBP in all SLBP mutants except S20A/S23A SLBP. HEK293 cells were treated with control or Pin1 siRNA, followed by cotransfection of Flag-tagged WT or mutant SLBP forms with $(His)_6$-tagged ubiquitin. The ubiquitinated proteins were purified over a nickel column as described in Materials and Methods. The lysates were probed for the presence of SLBP using the anti-SLBP antibody. A significant accumulation of ubiquitinated SLBP was observed when Pin1 was knocked down by siRNA, and no ubiquitination of SLBP was observed for the S20A/S23A mutant in either control or Pin1 siRNA-treated cells. (E) Flag-tagged SLBP WT and mutants were transiently transfected into HEK293 cells. The SLBP was immunoprecipitated using the Flag antibody and probed for Flag-tagged SLBP and Pin1. Only the T171A/T60A/T61A triple mutant significantly abrogated the SLBP-Pin1 interaction, indicating that multisite phosphorylation at these sites is required for interaction with Pin1.

domain, the data suggest that a bipartite mode of recognition is likely. During S phase, Pin1 may interact with Ser20/Ser23 as well as T171, as the mass spectrometry data suggest.

To determine whether Pin1 affected SLBP ubiquitination by the ubiquitin-proteasome system, we treated HEK293 cells with the proteasome inhibitor ALLN in the presence and absence of PiB (Fig. 5A). Treatment with either ALLN, PiB, or both increased SLBP levels. To determine whether Pin1 played a role in SLBP polyubiquitination, we knocked down Pin1 using siRNA and cotransfected Flag-SLBP WT and His-tagged ubiquitin into these cells (Fig. 5B). We found that knockdown of Pin1 by siRNA also resulted in significant accumulation of polyubiquitinated SLBP. Therefore, there is an increase in the levels of free SLBP as well as polyubiquitinated SLBP in the cell when Pin1 is inhibited. The

same effect was observed when Pin1 was chemically inhibited with PiB in HEK293 cells that were cotransfected with HA-Ub and Flag-SLBP (Fig. 5C). When we performed ubiquitination assays using the SLBP mutants (Fig. 5D), we found that mutation of Ser20 and Ser23 to alanines in the SLBP N terminus completely blocked SLBP ubiquitination. This effect was observed in cells treated with control siRNA as well as Pin1 siRNA. It was also observed in the context of the S20A/S23A/T171A triple mutant. This result is intriguing, as we see significant enrichment of these phosphorylation sites by mass spectrometry when Pin1 is inhibited. These results suggest that Pin1 plays two distinct roles in regulating SLBP. First, it interacts with phosphorylated Thr171 to facilitate dissociation of the SLBP-RNA complex, and second, it interacts with Ser/Thr-Pro sequences in the N terminus that include Ser20, Ser23, and possibly Thr60 and Thr61 to regulate SLBP polyubiquitination. Since we observed SLBP polyubiquitination in the Thr60/Thr61 double mutant, our data suggest that the Ser20/Ser23 site in the N terminus is the major phosphodegron for SLBP ubiquitination in asynchronous cells.

Pin1 knockdown promotes nuclear localization of SLBP. Human SLBP is a cell cycle-regulated protein (58), accumulating during the S phase of the cell cycle when histones are synthesized and DNA synthesis occurs. SLBP is found in both the nucleus and the cytoplasm during S phase (9). In the nucleus, SLBP is required for histone pre-mRNA processing (6), whereas in the cytoplasm, SLBP is important for histone protein synthesis (47) and is associated with histone mRNA. Inhibition of DNA replication results in a degradation of histone mRNA and a relocalization of SLBP to the nucleus (57).

To determine the role of T171 phosphorylation of SLBP in mammalian cells, we transiently transfected HA-tagged wild-type and T171A, T171D, and T171E human SLBP mutants into HeLa cells and determined the localization of the HA-tagged SLBP in asynchronously growing HeLa cells using a monoclonal anti-HA antibody. To distinguish between S-phase cells and cells in the G_1/G_2 phases of the cell cycle, we pulse-labeled the transfected HeLa cells with the nucleoside analog 5-ethynyl-2′-deoxyuridine (EdU) (as described in Materials and Methods) and immunolabeled the sites of EdU incorporation using the Click-iT 488 EdU kit (see Materials and Methods). Since EdU is incorporated only into single-stranded DNA, only S-phase cells are labeled (5). In addition, the spatial distribution of EdU-containing fluorescent foci in the cell nucleus allows one to distinguish between early-S-, mid-S-, and late-S-phase cells (A. Fritz and R. Berezney, unpublished results), as previously determined following bromodeoxyuridine incorporation (5, 42). The levels of the transiently transfected HA-SLBP wild type and mutants were similar to that of endogenous SLBP by Western blotting. Wild-type HA-SLBP was cell cycle regulated in a manner similar to that reported in previous studies (9, 58) (Fig. 6A). HA-SLBP was predominantly nuclear throughout the cell cycle and was only present in S-phase cells (58). In mid-S-to late-S-phase cells, some cytoplasmic staining was also observed, consistent with reports that SLBP participates in histone mRNA translation in the cytoplasm (Fig. 6A; see also Fig. S3 in the supplemental material) (47, 57). In contrast to findings for the wild-type SLBP, a significant number of non-S-phase cells showed high levels of T171A mutant SLBP (see Fig. S3 in the supplemental material). The T171A mutant was significantly more cytoplasmic in these cells (Fig. 6A; also see Fig. S3), suggesting that phosphorylation of SLBP at T171 is required for its efficient import into the nucleus. In contrast, the T171D and T171E SLBP mutants were almost exclusively nuclear throughout the cell cycle and were also present in cells that were not in S phase (did not stain for EdU), suggesting that T171 dephosphorylation is essential for the regulated degradation of SLBP in the nucleus at the end of S phase (Fig. 6A).

To determine the effect of Pin1 on SLBP localization, we examined the localization of endogenous SLBP and Pin1 in control and Pin1 siRNA-treated HeLa cells (Fig. 6B). Pin1 was found to be predominantly nuclear in HeLa cells and the fluorescence intensity was dramatically attenuated in the siRNA-treated cells, as expected. Since Pin1 is known to localize in nuclear speckles (44), we also probed for SC-35, a splicing factor that accumulates in speckles. Pin1 knockdown had no effect on speckle formation based on the SC-35 staining, indicating that the nuclear structure remains relatively unchanged in these cells. A significantly higher fluorescent signal was observed for endogenous SLBP in the nucleus that persisted throughout the cell cycle, similar to the localization of the T171D and T171E mutants (Fig. 6B). We also probed for the HA tag in HeLa cells that were stably transfected with HA-SLBP and obtained results identical to those with the endogenous protein (Fig. 6C). Intriguingly, CPSF160, which is also stabilized in response to the Pin1 siRNA, accumulates in the nucleolus in these cells (Fig. 6B).

The high-resolution microscopy images provided qualitative evidence that a Pin1 knockdown resulted in increased nuclear accumulation of both endogenous SLBP and HA-SLBP in HeLa cells that stably express HA-SLBP. A drawback of microscopy is that the interpretation of increased nuclear accumulation is based solely on visual analysis of 50 to 100 cells. To obtain statistically significant data, we used ImageStream (IS) flow cytometry, which combines the strength of flow cytometry with microscopy (39). In this analysis, cells are stained for SLBP-FITC (to stain for the endogenous SLBP in untransfected cells) as well as DRAQ5, a nucleus-specific stain. The FITC and DRAQ5 fluorescence is simultaneously imaged, and at least 5,000 events are captured for control and treated cells. A similarity score (SS), which is the log-transformed Pearson's correlation coefficient between the pixel values of the FITC and DRAQ5 image pairs, reflects the degree of nuclear accumulation of SLBP. Looking at the distribution histograms for the similarity score (Fig. 6D), a higher similarity score indicates that there is strong correlation between the signal intensity distribution of SLBP and DRAQ5 in the nucleus associated with nuclear localization of SLBP, and conversely, a shift to the left means a weaker correlation, associated with a more cytoplasmic distribution of SLBP. The mean similarity score for the control population of HeLa cells was −0.26, and that for Pin1 siRNA-treated HeLa cells was 0.8. An increase in SLBP fluorescence was also observed in the knockdown (mean fluorescence intensity was 65,000 for the Pin1 siRNA-treated cells versus 58,000 for the control). Therefore, the IS data indicate that there is an increase in SLBP levels in Pin1 siRNA-treated cells, and the excess SLBP is compartmentalized in the nucleus. Taken together, these studies demonstrate that downregulating Pin1 results in increased accumulation of SLBP in the nucleus, mimicking the localization of the phosphomimetic T171E and T171D SLBP mutants.

Downregulation of Pin1 activity increases histone mRNA abundance and stability. To understand the effects of Pin1 on regulation of histone mRNA abundance, we knocked down Pin1 using RNA interference (RNAi) in HeLa cells and HEK293 cells

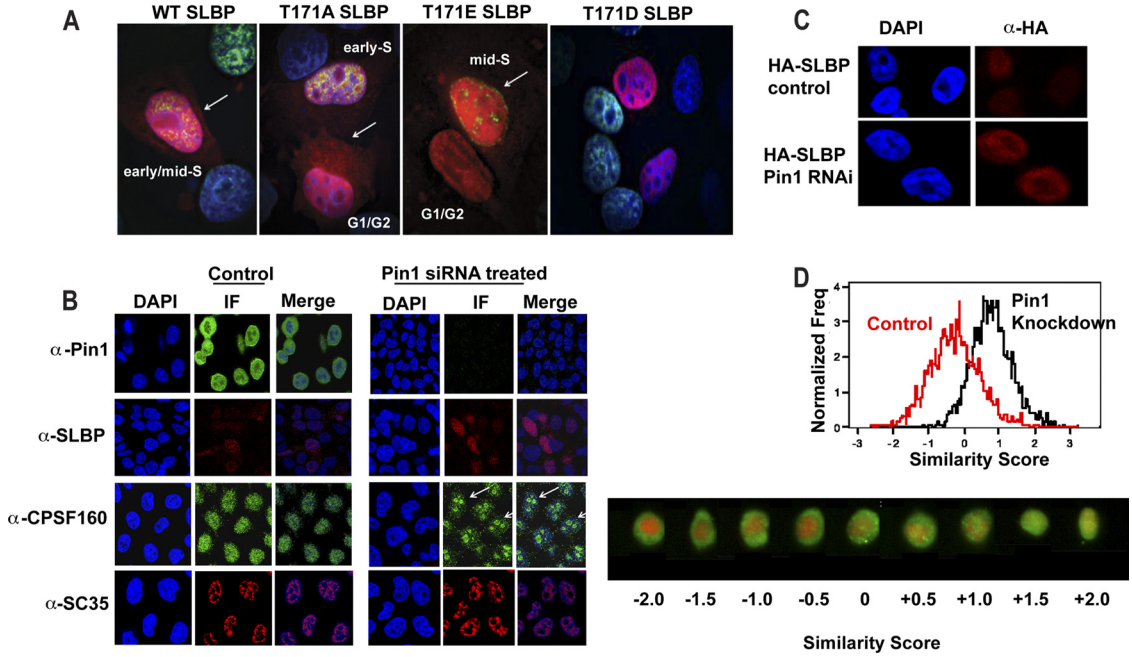

FIG 6 Localization of SLBP T171 mutants and SLBP in Pin1 siRNA-treated cells. (A) The distribution of SLBP wild type and T171A and T171E mutants in HeLa cells was visualized in 0.5-μm optical sections following deconvolution. The SLBP is shown in red, the DAPI in blue, and the EdU in green. The first image in panel A shows a cell in early-mid-S phase with WT SLBP present predominantly in the nucleus, but some SLBP is also in the cytoplasm. The second panel shows two cells with T171A SLBP staining. One cell is in early S phase and shows nuclear and some cytoplasmic staining. The second cell is not in S phase and shows an abundance of T171A SLBP in the cytoplasm. The third and fourth panels show the localization of T171E and T171D SLBPs, which is predominantly nuclear in both S-phase and non-S-phase cells. The individual staining patterns are shown in Fig. S3 in the supplemental material. (B) Representative confocal microscopic section images of control HeLa cells (left) and Pin1 siRNA-treated HeLa cells (right) that were stained with DAPI for nuclear imaging (in blue). Immunofluorescence (IF) for Pin1, SLBP, CPSF160, and SC-35 is shown in red or green, and the merge panel is shown on the right of each data set. siRNA knockdown of Pin1 results in increased fluorescence intensity in the nucleus for SLBP, whereas CPSF160 partitions into the nucleoli. There is no change in speckle formation as determined by the localization of SC-35 foci. (C) HeLa cells stably expressing HA-SLBP were probed to confirm the increase in nuclear signal observed in Pin1 siRNA-treated cells. HA-SLBP is shown in red, and DAPI is shown in blue. Representative confocal sections are displayed. (D) ImageStream analysis of control and Pin1 siRNA-treated HeLa cells. Similarity score distributions as a measure of SLBP nuclear distribution for control HeLa cells (red) and Pin1 knockdown cells (black) are shown. Representative composite images of SLBP (green) and DRAQ5 (red) corresponding to similarity scores are shown below.

and analyzed the total RNA by qRT-PCR. Intriguingly, all five core replication-dependent histone mRNAs (H1, H2A, H2B, H3, and H4) showed increased mRNA abundance in Pin1 RNAi-treated cells (Fig. 7A). The observed increase in abundance is between 1.3- and 3.0-fold (Fig. 7A) for H2A, H2B, H3, and H4. Since histone mRNAs are expressed only during S phase, and Pin1 RNAi knockdown cells show fewer S-phase cells (Fig. 3E), this represents approximately a 1.7- to 4.0-fold change in histone mRNA abundance overall. This apparently modest change in steady-state mRNA levels is biologically significant, since previous studies report 2- or 3-fold changes in histone mRNA steady-state levels as a result of alterations in regulated decay pathways that affect histone mRNA turnover (20, 48). A similar increase in histone mRNA abundance was observed when HEK293 cells were treated with the PiB inhibitor (Fig. 7B). The increase in histone mRNA levels was restored to control levels when Pin1 was overexpressed in siRNA-treated cells (Fig. 7C). Surprisingly, overexpression of the Pin1 W34A mutant, which is considered to be binding defective toward Pin1 substrates, also restored histone mRNA levels (Fig. 7C), indicating either that overexpression of this mutant is sufficient to compensate for the decreased binding or that W34 does not play a critical role in interaction with SLBP. In addition, a 2-fold increase in histone mRNA levels was observed when SLBP WT or SLBP T171E was transfected into the control and siRNA-treated cells. However, histone mRNA levels were reduced by 40 to 50% in the context of T171A SLBP (Fig. 7C). These experiments demonstrate that the observed effects on histone mRNA levels are due to the prolyl isomerase activity of Pin1 on the T171-Pro172 site of human SLBP.

To determine whether the observed increase in histone mRNA abundance was due to decreased rate of decay of the histone mRNA, we synchronized HEK293 cells by double-thymidine block and measured the histone mRNA levels cells after addition of hydroxyurea (HU) in the presence and absence of PiB (Fig. 7D). Addition of HU triggers histone mRNA decay due to inhibition of DNA synthesis. Cells were harvested every 15 min for 1.5 h after addition of HU, and the mRNA levels of histone H1, H4, H2A,H2B, and H3 were quantified by RT-PCR. The data suggest that the increased abundance of the histone mRNAs due to inhibition of Pin1 with PiB was due to a decreased rate of decay (Fig. 7D). Therefore, Pin1 affects histone mRNA stability.

Together, these data suggest that Pin1 is involved at multiple steps in SLBP function and hence in the regulation of histone mRNAs in the cell.

DISCUSSION

In this study, we have shown that SLBP is a substrate for Pin1 *in vivo* and that histone mRNA abundance and SLBP levels are al-

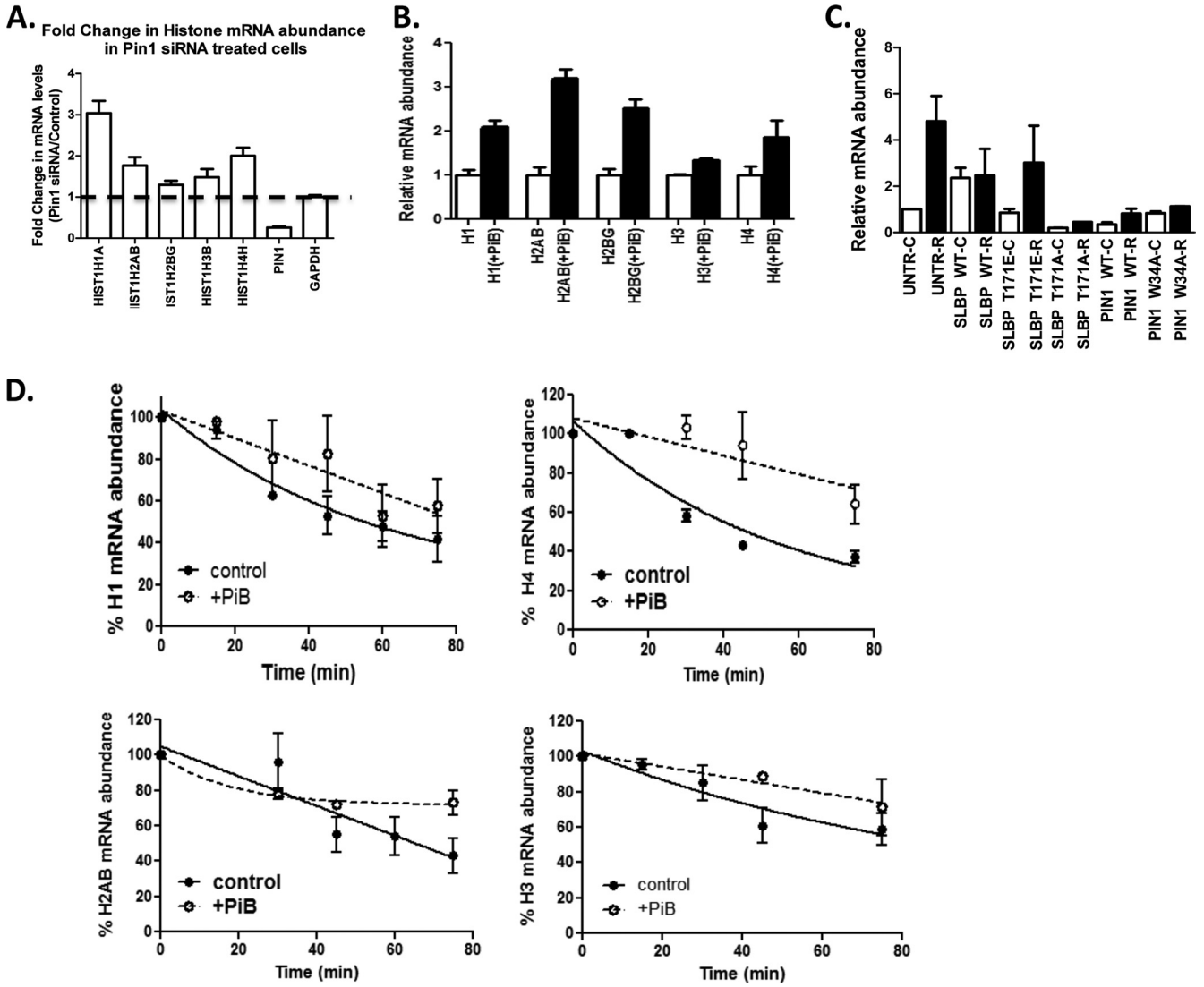

FIG 7 Effect of Pin1 inhibition on histone mRNA levels. (A) HeLa cells were treated with 50 nM Pin1 siRNA for 72 h. The change in histone mRNA abundance measured after Pin1 knockdown was validated by RT-PCR for five core histone genes, Pin1, and GAPDH. The average fold change determined from the C_T values using the comparative C_T method is depicted with the standard errors derived from three independent data sets. (B) The effect of chemical inhibition of Pin1 by the PiB inhibitor on histone gene abundance was determined in HEK293 cells by RT-PCR. The experiment was performed in triplicate. (C) HEK293 cells were treated with either control siRNA (designated with a "-C" extension) or Pin1 siRNA (designated with an "-R" extension). Forty-eight hours after the second hit, the cells either were left untransfected (UNTR) or were transfected with SLBP WT or the SLBP T171E or SLBP T171A mutant or Pin1 WT or the Pin1 W34A mutant as indicated. The cells were harvested after 24 h, and the histone mRNA abundance for HIST1 H4 was quantified by RT-PCR as described in Materials and Methods. (D) mRNA decay rates for four different histone mRNAs measured after the addition of hydroxyurea in the presence and absence of PiB in HEK293 cells. The experiments were done in triplicate. The mRNA was quantified for each time point using RT-PCR.

tered when Pin1 is inhibited. Pin1 has also been shown to regulate the activity of AUF1 (10). There are a number of parallels in Pin1 regulation of histone mRNA metabolism via SLBP and the regulation of the GM-CSF mRNA decay via AUF1 (10). In eosinophils, all four isoforms of the ARE-binding protein AUF1 immunoprecipitate with Pin1 in cross-linking immunoprecipitation experiments, and Pin1 regulates the association of AUF1 with the GM-CSF mRNA *in vivo* (10, 50). AUF1 proteins were shown to associate with GM-CSF mRNA only when Pin1 was inhibited with juglone, whereas Pin1 activation by hyaluronic acid abolished binding of AUF1 to the GM-CSF mRNA. Since AUF1 recruits the exosome via direct interactions with PM-Scl-75, it was suggested that removal of AUF1 would lead to stabilization of the mRNA. Intriguingly, the decay of the GM-CSF mRNA is also linked to the proteasome pathway (30, 31). Overexpression of deubiquinating enzymes directly affects the half-life of the GM-CSF mRNA, although the protein targets that mediate this effect have not been identified.

We have shown using fluorescence and EMSA that the direct interaction of phosphorylated SLBP with Pin1 can dissociate the SLBP-histone mRNA complex *in vitro*, particularly when the reaction is carried out in the presence of PP2A. Pin1 binds SLBP in its RNA binding domain at a conserved TPNK sequence; phosphorylation of *Drosophila* SLBP (dSLBP) at this site (T230 in

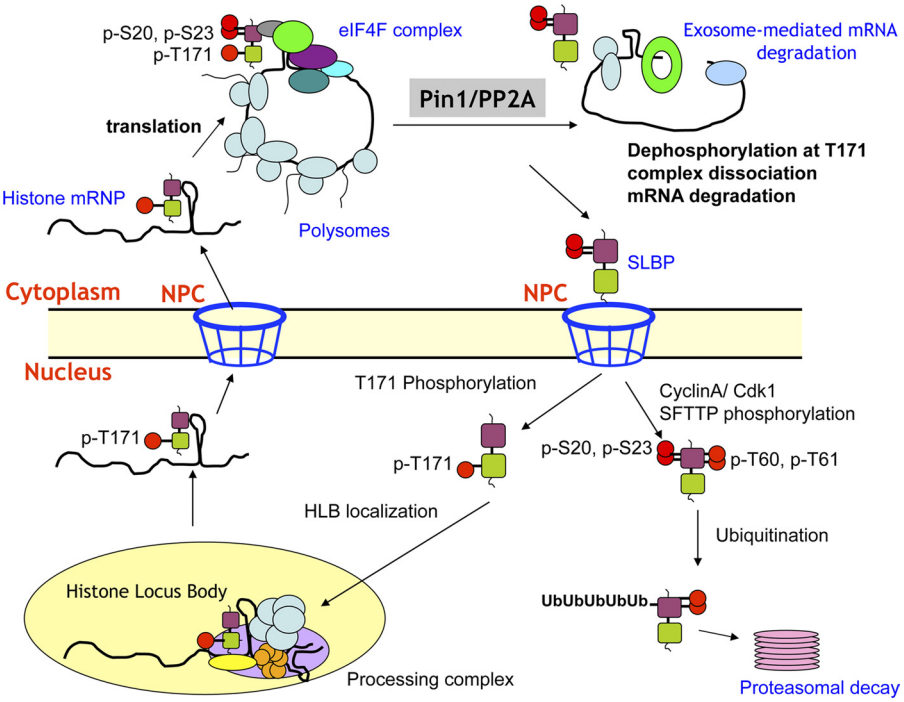

FIG 8 Model for the role of Pin1 in regulating histone mRNA decay. Our data suggest that T171 phosphorylation is required for efficient import of SLBP into the nucleus during S phase. During S phase and at the end of S phase, Pin1 acts with a phosphatase such as PP2A to dephosphorylate SLBP, thereby dissociating SLBP from the histone message in the cytoplasm. Pin1 may also regulate SLBP phosphorylation at the N terminus at Ser20 and Ser23, which we have identified as a phosphodegron that controls SLBP polyubiquitination. At the end of S phase, SLBP is also phosphorylated at Thr60 and Thr61, which is reported to trigger SLBP degradation (67). The histone mRNA is consequently degraded in the cytoplasm, whereas SLBP is degraded by the ubiquitin-proteasome pathway in the nucleus.

dSLBP) is essential for viability of *Drosophila* embryos and for histone pre-mRNA processing, and the mutant protein is not imported into the nucleus (29). Transgenic flies that harbor a T-to-A mutation at position 230 in dSLBP are unable to rescue the *Slbp* null mutant phenotype, and the histone message is misprocessed *in vivo* and is polyadenylated (29). We have shown that phosphorylation of T171 in human SLBP (the equivalent of T230 in dSLBP) also affects subcellular localization of human SLBP, although it does not have the dramatic effect as seen with the *Drosophila* protein. More of the T171A SLBP mutant is in the cytoplasm than wild-type SLBP, whereas the phosphomimetic mutants T171D SLBP and T171E SLBP are predominantly nuclear. Knockdown of Pin1 also results in increased accumulation of SLBP in the nucleus, the likely site of SLBP degradation. In addition, we have identified Ser20 and Ser23 in the sequence $S^{20}PPS^{23}P$ as two new phosphorylation sites that appear to be critical for SLBP polyubiquitination. These sites may correspond to a phosphodegron that is critical for polyubiquitination of SLBP during S phase and possibly also at the end of S phase. Phosphorylation at these sites is sensitive to Pin1 inhibition, and mutation of Ser20 and Ser23 to alanines blocked SLBP polyubiquitination. In contrast, no inhibition of polyubiquitination was observed when the SFTTP sequence was mutated to alanines in our study.

Knockdown or inhibition of Pin1 also results in increased abundance of histone mRNAs, at least partly due to stabilization of histone mRNA. Taken together, our data suggest a model that is summarized in Fig. 8. We propose that T171 phosphorylation is important for high-affinity binding to the stem-loop necessary for recruitment of SLBP to the site of histone pre-mRNA processing in the nucleus. During S phase, SLBP remains phosphorylated at T171 and accompanies the histone mRNP to the cytoplasm, where it is important for translation of the histone mRNA. Dephosphorylation of SLBP in its RNA binding domain by Pin1 and a phosphatase is likely to be necessary for removal of SLBP from the histone 3′ UTR at the end of S phase, resulting in decay of histone mRNAs, and for subsequent proteasomal degradation of SLBP. It is likely that inhibition of Pin1 decreases the rate of removal of SLBP from the histone message, thereby stabilizing the mRNA. The role of phosphorylation of S20 and S23 may be to regulate proteasomal degradation of SLBP during S phase. The SLBP that is released from the histone mRNP in the cytoplasm may reenter the nucleus, where it may be recycled or degraded. At the end of S phase, SLBP is phosphorylated by cyclin A/Cdk1, which either triggers rapid degradation of SLBP by the proteasome (23) or retains SLBP in the nucleus, thereby promoting its degradation. Cdk1 has previously been shown to phosphorylate HuR, enhancing nuclear accumulation of HuR during G_2 phase (21). The kinases that phosphorylate SLBP at Ser20, Ser23, and Thr171 remain unknown. Additional studies are also required to identify the E3 ligase(s) that interacts with SLBP and to determine the pathway of SLBP degradation in the nucleus and how it may affect other nuclear events such as histone pre-mRNA processing or export of the histone messenger ribonucleoprotein (mRNP) to the cytoplasm.

An interesting paradox in our study is that both histone mRNA levels and SLBP levels were significantly increased, although we had 30% fewer cells in S phase following downregulation or inhibition of Pin1 activity. Since normally both histone mRNAs and

SLBP are expressed at high levels only in S-phase cells, this suggests either that there is more histone mRNA and SLBP per S-phase cell or that histone mRNAs are no longer cell cycle regulated and persist in the G_1 and/or G_2 phase of the cell cycle. SLBP is the only factor whose levels are cell cycle regulated in a manner similar to that of histone mRNA, raising the possibility that the levels of SLBP and histone mRNA are coupled. However, current evidence suggests otherwise. Histone mRNA levels respond to signals regulating DNA replication, whereas SLBP levels respond to cell cycle signals. At the G_1/S border, there is a large amount of SLBP, but there is no histone mRNA (58). Similarly, SLBP degradation at the end of S phase is not required for histone mRNA degradation. It has been shown (67) that mutation of the SFTTP sequence that results in a stable form of SLBP that persists into G_2 phase has no effect on the degradation of histone mRNA, which degrades at the right time and with the same kinetics as is observed for endogenous SLBP-expressing cells. Conversely, when histone mRNAs are treated with inhibitors of DNA replication, the histone mRNA is degraded, although SLBP is stable (33, 58).

How might we explain the increased levels of both histone mRNA and SLBP in Pin1 knockdown cells? Our data suggest that Pin1 acts at the rate-limiting step required for degradation of both SLBP and histone mRNA, i.e., the dissociation of the SLBP from the histone mRNA stem-loop. Regardless of the signals that regulate histone mRNA and SLBP levels in the nucleus and cytoplasm, the histone mRNP must be remodeled at the end of S phase to ensure efficient degradation of the histone mRNA and reentry of the SLBP into the nucleus for ubiquitination and proteasomal decay. Failure to dissociate the SLBP-histone mRNA complex would affect both processes.

Pin1 has been reported to have both tumor-promoting and inhibitory roles in cancer progression (32, 35, 52). Since a number of Pin1 targets such as cyclin D, cyclin E, c-Myc, p53, p73, Raf kinase, Cdc25, and Jun are cell cycle-regulated proteins whose function is altered in tumorigenesis, Pin1 levels may promote uncontrolled growth of cancer cells via multiple signaling pathways. Our studies add yet another mechanism by which loss of Pin1 function may impact uncontrolled proliferation in cancer. We show that loss of Pin1 results in increased histone mRNA levels that are likely to impact chromatin function outside S phase. Increased levels of core histone proteins outside S phase could compete with the deposition of variant H2A and H3 histones, thereby having profound consequences, altering chromatin function and dynamics and having a more global effect on transcription, DNA repair, and chromosome segregation.

In summary, we have shown that the half-lives of histone mRNAs and the associated RNA binding protein SLBP are directly influenced by Pin1 activity. Pin1 regulates SLBP stability, ubiquitination, and localization and histone mRNA stability by playing an essential role in remodeling the histone mRNP at the end of S phase, when SLBP is required to dissociate from the histone message for efficient mRNA decay. We propose that Pin1 may use a similar mechanism to control the stability of a subset of eukaryotic mRNAs that are inherently unstable by targeting their associated RNA binding proteins.

ACKNOWLEDGMENTS

These studies were supported by NIH grant 1RO1-GM076660 to William F. Marzluff and Roopa Thapar and HWI faculty start-up funds to Roopa Thapar. Ronald Berezney and Andrew Fritz were supported by NIH grant 1RO1-GM072131.

The flow cytometry, ImageStream flow cytometry, and confocal microscopy were performed at RPCI's Flow and Image Cytometry Facility, the CCD microscopy and deconvolution image analysis were performed at the University at Buffalo, and the RT-PCR studies were performed at Hauptman-Woodward Institute and the UB Center of Excellence in Bioinformatics and Life Sciences (COE). The NMR studies were performed at the Biomolecular NMR Facility at the University of North Carolina at Chapel Hill. All other studies were performed at HWI. We thank Anthony Means (Duke University) for bacterial expression vectors for human and *Xenopus* Pin1 and Dirk Bohmann (University of Rochester) for mammalian expression vectors of HA and $(His)_6$-tagged ubiquitin. We also appreciate Mary LoPresti and Jean Kanyo (W. M. Keck Foundation Biotechnology Resource Laboratory, Yale University) for assistance with sample preparation and collecting some of the mass spectrometry data on the Orbitrap Elite (1S10 RR031795-0).

We declare that we have no financial or other conflicts of interest associated with this work.

REFERENCES

1. **Albert A, Lavoie S, Vincent M.** 1999. A hyperphosphorylated form of RNA polymerase II is the major interphase antigen of the phosphoprotein antibody MPM-2 and interacts with the peptidyl-prolyl isomerase Pin1. J. Cell Sci. **112**(Part 15):2493–2500.
2. **Alterman RB, et al.** 1984. Cell cycle regulation of mouse H3 histone mRNA metabolism. Mol. Cell. Biol. **4**:123–132.
3. **Borchers CH, et al.** 2006. Combined top-down and bottom-up proteomics identifies a phosphorylation site in stem-loop-binding proteins that contributes to high-affinity RNA binding. Proc. Natl. Acad. Sci. U. S. A. **103**:3094–3099.
4. **Crenshaw DG, Yang J, Means AR, Kornbluth S.** 1998. The mitotic peptidyl-prolyl isomerase, Pin1, interacts with Cdc25 and Plx1. EMBO J. **17**:1315–1327.
5. **Dimitrova DS, Berezney R.** 2002. The spatio-temporal organization of DNA replication sites is identical in primary, immortalized and transformed mammalian cells. J. Cell Sci. **115**:4037–4051.
6. **Dominski Z, Erkmann JA, Greenland JA, Marzluff WF.** 2001. Mutations in the RNA binding domain of stem-loop binding protein define separable requirements for RNA binding and for histone pre-mRNA processing. Mol. Cell. Biol. **21**:2008–2017.
7. **Dominski Z, et al.** 2002. 3′ end processing of Drosophila melanogaster histone pre-mRNAs: requirement for phosphorylated Drosophila stem-loop binding protein and coevolution of the histone pre-mRNA processing system. Mol. Cell. Biol. **22**:6648–6660.
8. **Dougherty MK, et al.** 2005. Regulation of Raf-1 by direct feedback phosphorylation. Mol. Cell **17**:215–224.
9. **Erkmann JA, et al.** 2005. Nuclear import of the stem-loop binding protein and localization during the cell cycle. Mol. Biol. Cell **16**:2960–2971.
10. **Esnault S, Shen ZJ, Whitesel E, Malter JS.** 2006. The peptidyl-prolyl isomerase Pin1 regulates granulocyte-macrophage colony-stimulating factor mRNA stability in T lymphocytes. J. Immunol. **177**:6999–7006.
11. **Finn G, Lu KP.** 2008. Phosphorylation-specific prolyl isomerase Pin1 as a new diagnostic and therapeutic target for cancer. Curr. Cancer Drug Targets **8**:223–229.
12. **Gnad F, Gunawardena J, Mann M.** 2011. PHOSIDA 2011: the posttranslational modification database. Nucleic Acids Res. **39**:D253–D260.
13. **Greenwood AI, et al.** 2011. Complete determination of the Pin1 catalytic domain thermodynamic cycle by NMR lineshape analysis. J. Biomol. NMR **51**:21–34.
14. **Haupt Y.** 2004. p53 regulation: a family affair. Cell Cycle **3**:884–885.
15. **Heintz N, Sive HL, Roeder RG.** 1983. Regulation of human histone gene expression: kinetics of accumulation and changes in the rate of synthesis and in the half-lives of individual histone mRNAs during the HeLa cell cycle. Mol. Cell. Biol. **3**:539–550.
16. **Hirosawa M, Hoshida M, Ishikawa M, Toya T.** 1993. MASCOT: multiple alignment system for protein sequences based on three-way dynamic programming. Comput. Appl. Biosci. **9**:161–167.
17. **Hutchins JR, Clarke PR.** 2004. Many fingers on the mitotic trigger: post-translational regulation of the Cdc25C phosphatase. Cell Cycle **3**:41–45.
18. **Jacobs DM, et al.** 2002. 1H, 13C and 15N backbone resonance assignment

of the peptidyl-prolyl cis-trans isomerase Pin1. J. Biomol. NMR **23**:163–164.
19. **Jacobs DM, et al.** 2003. Peptide binding induces large scale changes in inter-domain mobility in human Pin1. J. Biol. Chem. **278**:26174–26182.
20. **Kaygun H, Marzluff WF.** 2005. Regulated degradation of replication-dependent histone mRNAs requires both ATR and Upf1. Nat. Struct. Mol. Biol. **12**:794–800.
21. **Kim HH, et al.** 2008. Nuclear HuR accumulation through phosphorylation by Cdk1. Genes Dev. **22**:1804–1815.
22. **Kolev NG, Steitz JA.** 2005. Symplekin and multiple other polyadenylation factors participate in 3′-end maturation of histone mRNAs. Genes Dev. **19**:2583–2592.
23. **Koseoglu MM, Graves LM, Marzluff WF.** 2008. Phosphorylation of threonine 61 by cyclin a/Cdk1 triggers degradation of stem-loop binding protein at the end of S phase. Mol. Cell. Biol. **28**:4469–4479.
24. **Krishnamurthy S, Ghazy MA, Moore C, Hampsey M.** 2009. Functional interaction of the Ess1 prolyl isomerase with components of the RNA polymerase II initiation and termination machineries. Mol. Cell. Biol. **29**:2925–2934.
25. **Kumar R.** 2009. Pin1 regulates parathyroid hormone mRNA stability. J. Clin. Invest. **119**:2887–2891.
26. **Labeikovsky W, Eisenmesser EZ, Bosco DA, Kern D.** 2007. Structure and dynamics of Pin1 during catalysis by NMR. J. Mol. Biol. **367**:1370–1381.
27. **Landrieu I, et al.** 2010. NMR spectroscopy of the neuronal tau protein: normal function and implication in Alzheimer's disease. Biochem. Soc. Trans. **38**:1006–1011.
28. **Landrieu I, et al.** 2011. Molecular implication of PP2A and Pin1 in the Alzheimer's disease specific hyperphosphorylation of Tau. PLoS One **6**:e21521. doi:10.1371/journal.pone.0021521.
29. **Lanzotti DJ, et al.** 2004. Drosophila stem-loop binding protein intracellular localization is mediated by phosphorylation and is required for cell cycle-regulated histone mRNA expression. Mol. Biol. Cell **15**:1112–1123.
30. **Laroia G, Cuesta R, Brewer G, Schneider RJ.** 1999. Control of mRNA decay by heat shock-ubiquitin-proteasome pathway. Science **284**:499–502.
31. **Laroia G, Sarkar B, Schneider RJ.** 2002. Ubiquitin-dependent mechanism regulates rapid turnover of AU-rich cytokine mRNAs. Proc. Natl. Acad. Sci. U. S. A. **99**:1842–1846.
32. **Lee TH, Pastorino L, Lu KP.** 2011. Peptidyl-prolyl cis-trans isomerase Pin1 in ageing, cancer and Alzheimer disease. Expert Rev. Mol. Med. **13**:e21.
33. **Levine BJ, Chodchoy N, Marzluff WF, Skoultchi AI.** 1987. Coupling of replication type histone mRNA levels to DNA synthesis requires the stem-loop sequence at the 3′ end of the mRNA. Proc. Natl. Acad. Sci. U. S. A. **84**:6189–6193.
34. **Liu W, Youn HD, Zhou XZ, Lu KP, Liu JO.** 2001. Binding and regulation of the transcription factor NFAT by the peptidyl prolyl cis-trans isomerase Pin1. FEBS Lett. **496**:105–108.
35. **Lu KP.** 2004. Pinning down cell signaling, cancer and Alzheimer's disease. Trends Biochem. Sci. **29**:200–209.
36. **Lu KP, Finn G, Lee TH, Nicholson LK.** 2007. Prolyl cis-trans isomerization as a molecular timer. Nat. Chem. Biol. **3**:619–629.
37. **Lu KP, Hanes SD, Hunter T.** 1996. A human peptidyl-prolyl isomerase essential for regulation of mitosis. Nature **380**:544–547.
38. **Lu KP, Zhou XZ.** 2007. The prolyl isomerase PIN1: a pivotal new twist in phosphorylation signalling and disease. Nat. Rev. Mol. Cell Biol. **8**:904–916.
39. **Maguire O, Collins C, O'Loughlin K, Miecznikowski J, Minderman H.** 2011. Quantifying nuclear p65 as a parameter for NF-kappaB activation: correlation between ImageStream cytometry, microscopy, and Western blot. Cytometry A **79**:461–469.
40. **Marzluff WF, Wagner EJ, Duronio RJ.** 2008. Metabolism and regulation of canonical histone mRNAs: life without a poly(A) tail. Nat. Rev. Genet. **9**:843–854.
41. **Morris DP, Phatnani HP, Greenleaf AL.** 1999. Phospho-carboxyl-terminal domain binding and the role of a prolyl isomerase in pre-mRNA 3′-end formation. J. Biol. Chem. **274**:31583–31587.
42. **Nakayasu H, Berezney R.** 1989. Mapping replicational sites in the eucaryotic cell nucleus. J. Cell Biol. **108**:1–11.
43. **Pastorino L, et al.** 2006. The prolyl isomerase Pin1 regulates amyloid precursor protein processing and amyloid-beta production. Nature **440**:528–534.
44. **Pawlicki JM, Steitz JA.** 2009. Subnuclear compartmentalization of transiently expressed polyadenylated pri-microRNAs: processing at transcription sites or accumulation in SC35 foci. Cell Cycle **8**:345–356.
45. **Ranganathan R, Lu KP, Hunter T, Noel JP.** 1997. Structural and functional analysis of the mitotic rotamase Pin1 suggests substrate recognition is phosphorylation dependent. Cell **89**:875–886.
46. **Ritt DA, Monson DM, Specht SI, Morrison DK.** 2010. Impact of feedback phosphorylation and Raf heterodimerization on normal and mutant B-Raf signaling. Mol. Cell. Biol. **30**:806–819.
47. **Sànchez R, Marzluff WF.** 2002. The stem-loop binding protein is required for efficient translation of histone mRNA in vivo and in vitro. Mol. Cell. Biol. **22**:7093–7104.
48. **Sariban E, Wu RS, Erickson LC, Bonner WM.** 1985. Interrelationships of protein and DNA syntheses during replication of mammalian cells. Mol. Cell. Biol. **5**:1279–1286.
49. **Shaw PE.** 2007. Peptidyl-prolyl cis/trans isomerases and transcription: is there a twist in the tail? EMBO Rep. **8**:40–45.
50. **Shen ZJ, Esnault S, Malter JS.** 2005. The peptidyl-prolyl isomerase Pin1 regulates the stability of granulocyte-macrophage colony-stimulating factor mRNA in activated eosinophils. Nat. Immunol. **6**:1280–1287.
51. **Singh N, et al.** 2009. The Ess1 prolyl isomerase is required for transcription termination of small noncoding RNAs via the Nrd1 pathway. Mol. Cell **36**:255–266.
52. **Takahashi K, Uchida C, Shin RW, Shimazaki K, Uchida T.** 2008. Prolyl isomerase, Pin1: new findings of post-translational modifications and physiological substrates in cancer, asthma and Alzheimer's disease. Cell. Mol. Life Sci. **65**:359–375.
53. **Uchida T, et al.** 2003. Pin1 and Par14 peptidyl prolyl isomerase inhibitors block cell proliferation. Chem. Biol. **10**:15–24.
54. **Verdecia MA, Bowman ME, Lu KP, Hunter T, Noel JP.** 2000. Structural basis for phosphoserine-proline recognition by group IV WW domains. Nat. Struct. Biol. **7**:639–643.
55. **Wagner EJ, Garcia-Blanco MA.** 2002. RNAi-mediated PTB depletion leads to enhanced exon definition. Mol. Cell **10**:943–949.
56. **Werner-Allen JW, et al.** 2011. *cis*-Proline-mediated Ser(P)5 dephosphorylation by the RNA polymerase II C-terminal domain phosphatase Ssu72. J. Biol. Chem. **286**:5717–5726.
57. **Whitfield ML, et al.** 2004. SLBP is associated with histone mRNA on polyribosomes as a component of the histone mRNP. Nucleic Acids Res. **32**:4833–4842.
58. **Whitfield ML, et al.** 2000. Stem-loop binding protein, the protein that binds the 3′ end of histone mRNA, is cell cycle regulated by both translational and posttranslational mechanisms. Mol. Cell. Biol. **20**:4188–4198.
59. **Williams AS, Marzluff WF.** 1995. The sequence of the stem and flanking sequences at the 3′ end of histone mRNA are critical determinants for the binding of the stem-loop binding protein. Nucleic Acids Res. **23**:654–662.
60. **Xu YX, Manley JL.** 2007. New insights into mitotic chromosome condensation: a role for the prolyl isomerase Pin1. Cell Cycle **6**:2896–2901.
61. **Xu YX, Manley JL.** 2007. Pin1 modulates RNA polymerase II activity during the transcription cycle. Genes Dev. **21**:2950–2962.
62. **Xu YX, Manley JL.** 2004. Pinning down transcription: regulation of RNA polymerase II activity during the cell cycle. Cell Cycle **3**:432–435.
63. **Yeh ES, Lew BO, Means AR.** 2006. The loss of PIN1 deregulates cyclin E and sensitizes mouse embryo fibroblasts to genomic instability. J. Biol. Chem. **281**:241–251.
64. **Yeh ES, Means AR.** 2007. PIN1, the cell cycle and cancer. Nat. Rev. Cancer **7**:381–388.
65. **Zhang M, Lam TT, Tonelli M, Marzluff WF, Thapar R.** 2012. Interaction of histone mRNA hairpin with stem-loop binding protein and regulation of the SLBP-RNA complex by phosphorylation and proline isomerization. Biochemistry **51**:3215–3231.
66. **Zhang Y, et al.** 2007. Structural basis for high-affinity peptide inhibition of human Pin1. ACS Chem. Biol. **2**:320–328.
67. **Zheng L, et al.** 2003. Phosphorylation of stem-loop binding protein (SLBP) on two threonines triggers degradation of SLBP, the sole cell cycle-regulated factor required for regulation of histone mRNA processing, at the end of S phase. Mol. Cell. Biol. **23**:1590–1601.
68. **Zhou XZ, et al.** 2000. Pin1-dependent prolyl isomerization regulates dephosphorylation of Cdc25C and tau proteins. Mol. Cell **6**:873–883.